CHARACTERIZATION OF STRUCTURAL, OPTICAL AND ELECTRICAL PROPERTIES OF Ni DOPED ZnO THIN FILMS

By

Sanjoy Chandra Das
Roll No.: 1009143002 F
Session: October, 2009
MASTER OF PHILOSOPHY

DEPARTMENT OF PHYSICS
BANGLADESH UNIVERSITY OF ENGINEERING AND TECHNOLOGY,
DHAKA-1000, BANGLADESH.

DECLARATION

It is hereby declared that this thesis or any part of it has not been submitted elsewhere for the award of any degree or diploma.

SANJOY CHANDRA DAS
Roll No. 1009143002 F
Session: October, 2009


Dedicated
to
all of my family
members

CONTENTS

CHAPTER- V: EXPERIMENTAL RESULTS AND DISCUSSION

CHAPTER-VI: CONCLUSIONS AND SUGGESTION FOR FUTURE WORK

APENDIX

List of figures **Page No.**

List of Tables

ACKNOWLEDGEMENTS

Firstly, I express very much gratefulness to the Almighty, who gives me the strength and energy to fulfill this research work. There are lots of people I would like to thank for various reasons.

I would like to express my profound gratefulness to my respectable and honorable supervisor **Dr. Jiban Podder,** Professor, Department of Physics, Bangladesh University of Engineering & Technology (BUET), Dhaka, for his constant support, hand-on instructions, and efforts to establish internal and external cooperation throughout my study. He is a great materials scientist. It is my great honor to be his student. What I learned from him will benefit my whole life.

I am thankful to **Dr. Md. Mostak Hossain,** Professor and Head, Department of Physics, (BUET), Dhaka, for providing necessary facilities and supports to carry out this work.

I wish to express my gratefulness to **Prof. Dr. Md. Abu Hashan Bhuiyan** for his various help. I also like to thank all respected teachers: **Prof. Dr. A. K. M. Akther Hossain, Prof. Dr. Md. Feroz Alam Khan**, **Dr. Forhad Mina, Mr. Mohammad Jellur Rahman**, **Mr. Muhammed Samir Ullah**, for their kind help and valuable suggestions.

I would like to give my special thanks to **Dr. D. K. Saha,** Chief Scientific Officer and **Mr. Md. Al-Mamun**, Engineer, Materials Science Division, Atomic Energy Centre, Dhaka, for helping in taking SEM and EDX data.

I am very much grateful to **Prof. Dr. Md. Khalilur Rahman Khan** and his students **Mr. Alop and Mr. Polash,** Department of Physics, University of Rajshahi, for his kind help during the study of electrical property.

I am grateful to **Dr. Md. Abdul Gafur**, Senior Engineer, BCSIR Laboratories for UV-VIS spectroscopy measurements.

I am also thankful to Department of Physics and Engineering Physics, **University of Saskatchewan, Canada**, for giving permission for XRD measurements on my samples.

I would like to thank **Mr. Md. Khorshed Alam, Ms. Mahajabin Taskin, Dr. Ferdousi Akther, Ms. Farhana Khanam , Mr. Kamal Uddin Azad, Mr. Abul Hasnat, Ms. Tamjida Rahman Luna, Mr. Md. Arifur Rahaman, Mr. Anis Munshi,** for their sincere help to this work.

Finally, I need to thank all of my family members. I express my heartfelt gratitude to my father and other family members for their continuous support and encouragement during this research work.

I thank the authority of **Bangladesh University of Engineering & Technology** for providing financial support and **Ministry of Science and Technology, the People's Republic of Bangladesh** for providing **"NSICT Fellowship"** to this thesis work.

ABSTRACT

Zinc Oxide (ZnO) and Nickel (Ni) doped ZnO ($Zn_{1-x}Ni_xO$) thin films (x= 0%, 1%, 3%, 5%, 10%, 15%) have been prepared by spray pyrolysis method on to glass substrate at 300 ^{0}C. The structural, optical and electrical properties of the as-deposited films are studied in details.

The energy dispersive X-ray (EDX) data of the films were taken. EDX result reveals that the deposited films are very close to the nominal composition. The scanning electron microscope (SEM) micrographs of the $Zn_{1-x}Ni_xO$ films have been taken for different compositions deposited on glass substrate at the temperature 300 ^{0}C. The SEM micrographs of as-deposited films show deposition covers the substrate well.

X-ray diffraction pattern has been recorded on as-deposited $Zn_{1-x}Ni_xO$ thin films. The as-deposited film has a broad peak with six identified peaks indicating the films amorphous with crystalline in nature. Lattice constants have been calculated using the prominent peaks of (100) and (002) the average value obtained are a =3.22 Å and c=5.17 Å. Structure of the material has been identified as hexagonal. Grain size of thin film was determined from (100). Grain size of the film decreases with the increase of Ni concentration from (1%-5%) of Ni then increases slightly. A secondary phase of NiO has been observed in higher Ni concentration sample excess doping of Ni.

Various optical constants such as absorbance, transmittance, refractive index, extension coefficient and optical conductivity of the films have been studied. For different compositions of as-deposited $Zn_{1-x}Ni_xO$ films, the band gap varies from 3.38 to 2.80 eV. The electrical resistivity measurements were made on number of films from the room temperature up to 440K. The resistivity of the films gradually decreases with the increase of temperature, which indicates the semiconducting nature of the materials. Resistivity also decreases with the increasing doping concentration.

CHAPTER-I
GENERAL INTRODUCTION

CHAPTER-I
GENERAL INTRODUCTION

1.1 Introduction

Thin film technology is an important branch of physics. Thin film is a modern technology, which contributes various sectors of experimental physics. Thin films mean a thin layer or coating of a material on another material. The definition of thin film means a thin layer of solid material is deposited on the substrate. The thickness of the thin film is comparable with the mean free path of the conduction electron.

A solid crystalline material whose electrical conductivity is between that of a conductors and an insulator is known as a semiconductor. Good conductors have resistivity between 10^{-7} q m to 10^{-8} q m at room temperature while the resistivity of insulators is in the range 10^{10} q m and 10^{14} q m. Semiconductors fall in resistivity between 10^{-6} q m to 10^{7} q m. Pure semiconductors behave like insulators at 0 K, however at normal temperatures, in contrast to metals, semiconductors have a negative coefficient of resistance due to the increase in the concentration of charge carriers as the temperature rises. The conductivity of a semiconductor material can be varied under an external electrical field. Devices made from semiconductor materials are the foundation of modern electronics, including radio, computers, telephones, and many other devices. Semiconductor devices include the transistor, many kinds of diodes including the light-emitting diode (LED), laser diode (LD) [1], the silicon controlled rectifier, and digital and analog integrated circuits. Solar photovoltaic panels are large semiconductor devices that directly convert light energy into electrical energy [2].

The property of semiconductors that makes them most useful for constructing electronic devices is that their conductivity may easily be modified by introducing impurities into their crystal lattice. The process of adding controlled impurities to a semiconductor is known as doping. The amount of impurity, or dopant, added to an intrinsic (pure) semiconductor varies its level of conductivity. Doped semiconductors are often referred to as extrinsic. By adding impurity to pure semiconductors, the

electrical conductivity may be varied not only by the number of impurity atoms but also, by the type of impurity atom.

The materials chosen as suitable dopants depend on the atomic properties of both the dopant and the material to be doped. In general, dopants that produce the desired controlled changes are classified as either electron acceptors or donors. A donor atom that activates donates weakly bound valence electrons to the material, creating excess negative charge carriers. These weakly bound electrons can move about in the crystal lattice relatively freely and can facilitate conduction in the presence of an electric field. The donor atoms introduce some states under, but very close to the conduction band edge. Electrons at these states can be easily excited to the conduction band, becoming free electrons, at room temperature. Conversely, an activated acceptor produces a hole. Semiconductors doped with donor impurities are called n-type, while those doped with acceptor impurities are known as p-type. The n and p type designations indicate which charge carrier acts as the material's majority carrier. The opposite carrier is called the minority carrier, which exists due to thermal excitation at a much lower concentration compared to the majority carrier.

II-VI binary semiconductor nanomaterials have attracted much attention due to their potential technological applications such as storage devices, high-speed electronics, nanoelectronics, optoelectronic and solar cells devices. Zinc Oxide (ZnO) is one of promising material of II-VI group. Transitional metal doped semiconductors are called diluted magnetic semiconductors (DMS). The diluted magnetic semiconductors exhibit simultaneously ferromagnetic and semiconducting properties and focused on a new practical technology namely "spintronics" (spin-electronics). Ni doped ZnO has combine ferromagnetic order at room temperature with semiconducting properties for spintronic devices. Transistors operate by controlling the flow of carriers through the semiconductor by applied electric fields. Spin, on the other hand, is used for the magnetic data storage. The word "spin electronics" refers to devices that manipulate the freedom of spin degree [3]. In traditional electronic devices, charge and spin are used separately. Charge, on one hand, is used for the computing. A new generation of devices based on the manipulation of spins may have completely new functionality, therefore drastically improves the computation speed and reduces power consumption.

1.2 Properties of transparent zinc oxide

In materials science, Zinc oxide (ZnO) is often called II-VI semiconductor because zinc and oxygen belong to the 2^{nd} and 6^{th} groups of the periodic table, respectively. It usually appears as a white powder, nearly insoluble in water. Zinc oxide (ZnO) is a wide bandgap (3.4 eV at room temperature) semiconductor that is desirable for many applications. It is attractive for forming various forms of nanostructures, such as nanorods, nanowires, and nanobelts [4]. Transparent transistors fabricated from ZnO have been reported. With its high exciton binding energy, ZnO is a good candidate for room temperature UV lasers. Its large piezoelectric constant is promising for ultrasonic transducers. ZnO is transparent and electrically conductive, making it an ideal material for solar cell windows. The mineral form of ZnO can be found in nature and is known as Zincite. Zinc oxide has the hexagonal wurtzite structure.

ZnO nanomaterials are promising candidates for nanoelectronic, optoelectronic and solar cells devices [5]. Compared with other semiconductor materials, ZnO has higher exciton binding energy (60 meV), is more resistant to radiation, and is multifunctional with uses in the areas as a piezoelectric, ferroelectric and ferromagnetic. ZnO based semiconductor and nanowire devices are also promising for the integration on a single chip. So far, the various applications of ZnO nano-materials such as biosensors and UV detectors [6].

1.2.1 Some important physical properties of ZnO semiconductors are given below:

- Molecular formula: ZnO
- Crystal structure: Hexagonal
- Molecular weight (g/mole) : 81.4084
- Band gap : 3.4 eV (direct)
- Appearance : White solid
- Density (g/cm^3) : 5.606
- Melting point (°C) : å 1975
- Solubility in water (g/L) : 1.6 (at 28 °C)
- Dielectric constant : 8.5
- Lattice energy (Kcal/mole) : 965

1.2.2 Crystal structure zinc oxide

Zinc oxide crystallizes in three forms: hexagonal wurtzite, cubic zincblende, and the rarely observed cubic rocksalt. The wurtzite structure is most stable at ambient conditions and thus most common. The zincblende form can be stabilized by growing ZnO on substrates with cubic lattice structure. In both cases, the zinc and oxide centers are tetrahedral.

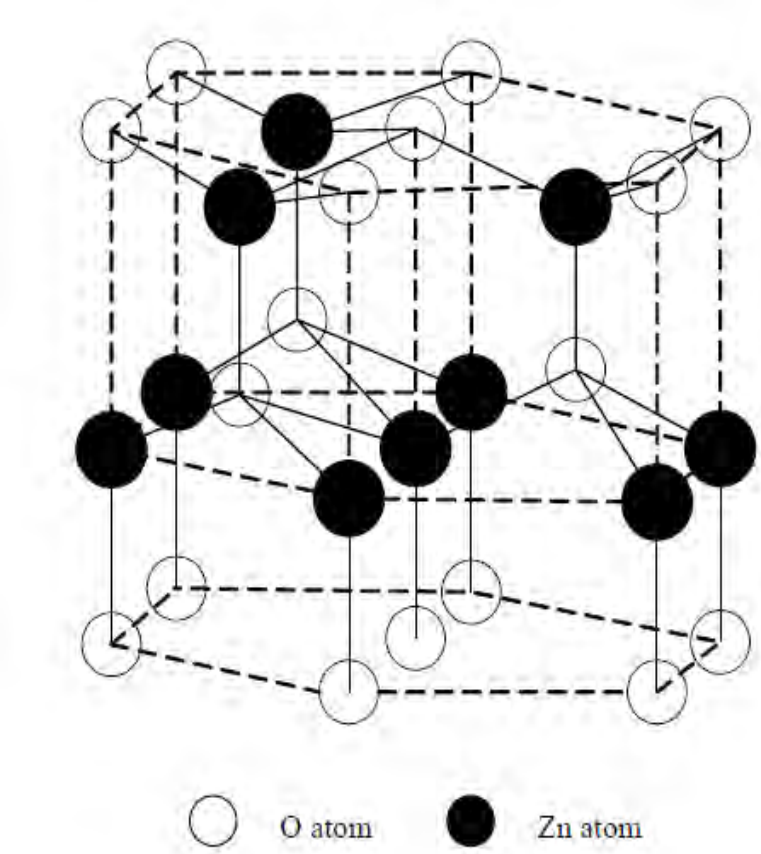

Fig.1.1: Hexagonal Wurtzite structure of ZnO

Hexagonal and zincblende polymorphs have no inversion symmetry . This and other lattice symmetry properties result in piezoelectricity of the hexagonal and zincblende ZnO [7].

1.3 Properties of Nickel

Nickel is a chemical element with the chemical symbol Ni and atomic number 28. The unit cell of nickel is a face centered cube with the lattice parameter of 0.352 nm giving an atomic radius of 0.124 nm. Nickel belongs to the transition metals and is hard, malleable, ductile, lustrous, silvery white, ferromagnetic metallic element in Group VIII of periodic table. Nickel is one of three noteworthy elements in the transition metals family (iron, cobalt, and nickel) that are known to produce a magnetic field. The electronic structure of Ni is $1s^2 2s^2 2p^6 3s 23p^6 3d^8 4s^2$. Its outer electrons shell has a $4s^2 3d^8$ configuration. While nickel can exist in oxidation states 0, +1, +2, +3, and +4, its only important oxidation state is 2 under normal environmental conditions. Nickel is a silvery-white metal with a slight golden tinge that takes a high polish. It is one of only four elements that are magnetic at or near room temperature. Its Curie temperature is 627K [8]. That is, nickel is non-magnetic above this temperature.

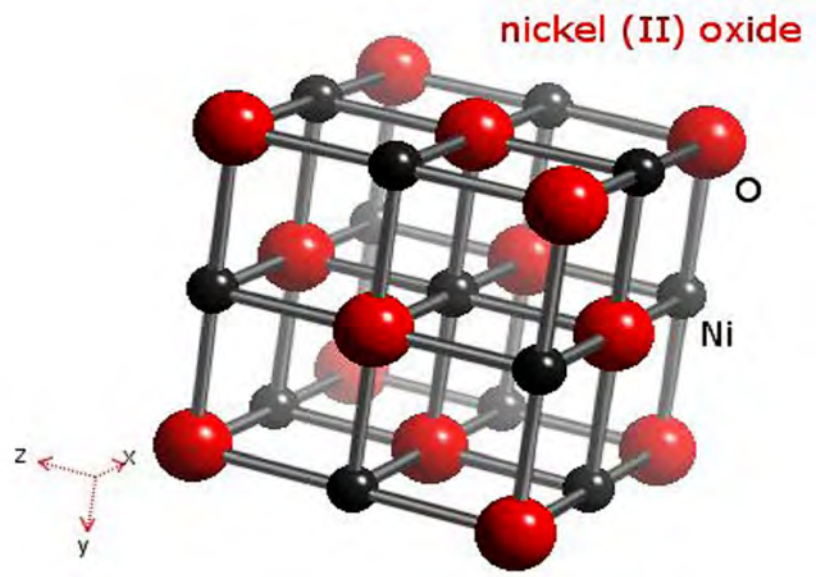

Fig.1.2: Crystal structure of nickel oxide

Nickel is used in many industrial and consumer products, including stainless steel, magnets, coinage, rechargeable batteries, electric guitar strings, microphone capsules, and special alloys. It is also used for plating and as a green tint in glass.

Nickel is pre-eminently an alloy metal, and its chief use is in the nickel steels and nickel cast irons, of which there are many varieties. It is also widely used in many other alloys, such as nickel brasses and bronzes, and alloys with copper, chromium, aluminium, lead, cobalt, silver, and gold.

1.3.1 Overview of nickel

- Atomic Number:28
- Series: Transition Metals
- Atomic Radius**:** 1.62Å
- Atomic Volume**:** 6.59cm^3/mol
- Covalent Radius**:** 1.15Å
- Crystal Structure**:** Cubic face centered
- Electrons per Energy Level**:** 2,8,16,2
- Ionic Radius**:** 0.69Å

1.4 Application of Thin Films

Thin films are widely used in todayôs technology, and their applications are expected to be even more widespread in future. It is not possible to give an exhaustive survey over thin film applications, but a listing may, nevertheless, be of some interest. The application areas for thin films are:

A. Optical function

1. Solar absorbing coatings
2. Anti- reflection layers on optical components
3. Coatings for laser optics
4. Display devices (CD)

B. Electrically functionl

1. Conductors, Insulators (resistors, capacitors)
2. Semiconductor, Super-conductors devices
3. Microelectronic devices
4. Solar cells

C. Magnetically function

1. Computer memories
2. Computer logic elements
3. Radio-frequency and microwave

D. Chemically function

1. Gas/liquid sensors

F. Decorative

1. Eyeglass frames
2. Costume jewelry

G. Optoelectronic applications:

Thin films are of current interest owing to their potential use in light emitting diodes and laser diodes. Besides this other photo-electronic device e.g., photovoltaic solar cells, photoconductive devices, light-emitting diodes, coatings, sensors, integrated components for telecommunication etc., are now under active consideration of the experimental physicists. In recent time popular utilization of this films as the absorber of the solar cells.

1.5 Diluted magnetic semiconductors

Transitional metal doped semiconductors are called diluted magnetic semiconductors (DMS) [9]. Transition metal doped II-VI compounds are the most common DMSs studied in the early period. DMS materials are semiconductors in which a fraction of the host cations can be substitutionally replaced by transition metal ions.

The partially filled 3d states contain unpaired electrons, which are responsible for localized magnetic moments. The diluted magnetic semiconductors exhibit simultaneously ferromagnetic and semiconducting properties [10] and focused on a new practical technology namely "spintronics" (spin-electronics). Spintronics is a new branch of electronics in which electron spin, in addition to charge, is manipulated to yield a desired electronic outcome. All spintronic devices act according to the simple scheme:

(1) Information is stored (written) into spins as a particular spin orientation (up or down),

(2) The spins, being attached to mobile electrons, carry the information along a wire, and

(3) The information is read at a terminal.

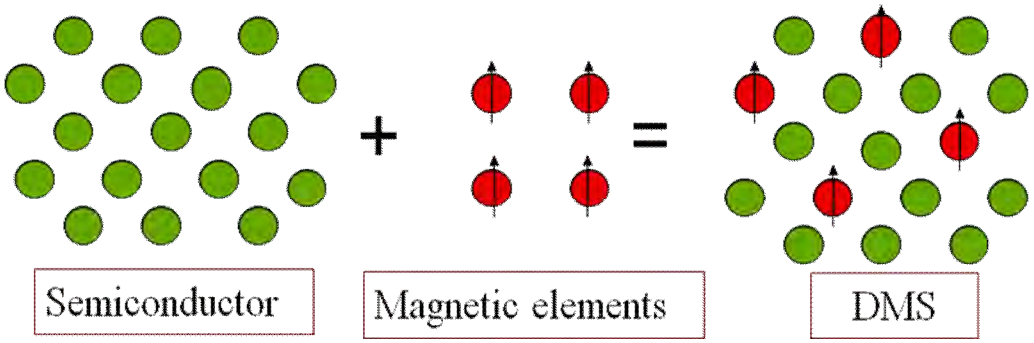

Spin orientation of conduction electrons survives for a relatively long time. which makes spintronic devices particularly attractive for memory storage and magnetic sensors applications and potentially for quantum computing where electron spin would represent a bit of information. It was in this context that the concept of diluted magnetic semiconductor (DMS) emerged. Examples of DMS: GaAs+Mn; TiO_2+Co; ZnO+Co; ZnO+Mn; ZnO+Ni etc.

1.6 Brief review of previous work

High purity ZnO films of different thicknesses were prepared using a Spray Pyrolysis deposition system at relatively low temperature (200 °C) and studied effect of surface morphology and optical properties of the as deposited thin films . From SEM study was observed nano fiber structure the undoped ZnO thin films [11]. Nanostructured ZnO thin films were deposited on glass by the dipcoating solï gel method and the photocatalytic activity of ZnO films is investigated [12].

Ni-doped ZnO nanostructures were synthesized through a pulsed-electro deposition-assisted chemical bath deposition method, and the optical and magnetic properties of the nanostructures were studied. The morphology of the nanostructures was observed by SEM rod like to a sheet like structure because of the different growth modes, and a growth mechanism is proposed to explain these findings. A strong UV emission

was observed for the nanorods. Ni was successfully doped into the ZnO wurtzite lattice structure as revealed by X-ray diffraction. Room temperature ferromagnetism was also observed in the Ni-doped ZnO nanostructures [13].

Nanocrystalline $Zn_{1-x}Ni_xO$ powders were synthesized by a simple solï gel autocombustion method using metal nitrates of zinc, nickel and glycine. Structural and optical properties of the Ni-doped ZnO samples were characterized using X-ray diffraction (XRD), scanning electron microscopy (SEM), energy dispersive analysis using X-rays (EDAX), UVï visible spectroscopy and photoluminescence (PL). X-ray diffraction analysis reveals that the Ni-doped ZnO crystallizes in a hexagonal wurtzite structure and secondary phase (NiO) was observed with the sensitivity of XRD measurement with the increasing nickel concentration [14].

Ni-doped ZnO films with different Ni Concentrations were prepared by radio-frequency magnetron sputtering and the structural, electrical and magnetic properties were studied of the films. The structural characterizations indicate that Ni ions in the 2+ valence state, uniformly distributed in the film, almost substitute for the Zn ions when x Ò 0.07, when x increases up to 0.11, a second phase Ni is formed. Room temperature ferromagnetism has been observed for all the Ni-doped ZnO wurtzite films [15].

Ni-doped comb-like ZnO semiconductor nanostructures have been synthesized by a simple chemical vapor-deposition method (CVD) at low temperature. The synthesized ZnO nanocombs consist of an array of very uniform, perfectly aligned, evenly spaced and long single-crystalline nanobelts (nanowires) with periods of about several tens of nanometers. XRD and Raman spectra results provide the evidence that Ni is incorporated into the ZnO lattice at Zn site. The ultraviolet emission intensity has been detected by photoluminescence spectra [16].

From the above review it is clear that Ni doped ZnO thin films have been prepared by various techniques and investigated different properties. But so far no details work have been reported on the ZnO thin films prepared by spray pyrolysis system. spray pyrolysis is very easy to handle and cost effective method. Considering the applications of ZnO thin films in various technologies we have decided to prepare Ni doped ZnO thin films by spray pyrolysis method and study various properties of the films.

1.7 Aim of the present work

In the recent years, the II-VI binary semiconductor nanomaterials have attracted much attention due to their potential technological applications such as storage devices, high-speed electronics, nanoelectronics, optoelectronic and solar cells devices [17]. ZnO is potentially useful because of attractive properties like non-toxicity, good electrical, optical and piezoelectric behavior [11]. Itôs wide band gap 3.4 eV makes it attractive for the development of light-emitting diodes, coatings, sensors, integrated components for telecommunication, solar cells, etc.[11]. The crystal structure of ZnO is hexagonal (a=3.2498, c=5.2066). Transitional metal doped semiconductors are called DMS. The diluted magnetic semiconductors exhibit simultaneously ferromagnetic and semiconducting properties and focused on a new practical technology namely "spintronics" (spin-electronics). It has vast demand for integrated optoelectronic applications such as light emitters and UV detectors [18]. Ni doped ZnO has combine ferromagnetic order at room temperature with semiconducting properties for spintronic devices such as magneto-optical devices and magnetic sensors applications. Small amount of Ni can make attractive effect of structural, optical and electrical properties of ZnO. This has motivated to investigate the influence of transition metals Ni dopants on the transport and optical properties of ZnO thin film in the present work. Although much work has been done on the electronic and optical properties of ZnO thin films but insufficient information is available on the $Zn_{1-x}Ni_xO$ thin films synthesized by spray pyrolysis deposition technique. Spray pyrolysis deposition technique is a simple, economical, viable technique and capable of producing good quality films for device application. From practical point of view, Ni doped II-VI compound semiconductor to be deposited on the glass substrate and to be studied

a) The surface morphology of the films.
b) The optical constants e.g. absorption coefficient, optical band gap(Eg), refractive index etc. to be determined by UV visible spectrophotometer.
c) The crystal structure of the deposited films to be analyzed by XRD .
d) Electrical conductivity measurement is to be carried out by Vander Pauw four probe method.

Reference

1. Lim B. J. H., Kang C. K., Kim K. K., Park L. K., Hwang D. K., and Park S. J., ñUV Electroluminescence Emission from ZnO Light-Emitting Diodes Grown by High-Temperature Radiofrequency Sputteringò Adv. Mater., Vol. 18, P. 2720ï 2724, 2006.

2. Fortunato E., Ginley D., Hosono H., and Paine D. C., ñTransparent Conducting Oxides for Photovoltaicsò MRS Bulletin, Vol. 32, P. 242-247, 2007.

3. Licu C., Yun, and Morkoc H.,òFerromagnetism of ZnO and GaN: A Reviewò J. of Mater. Sci: Mater. Electron. Vol. 16, P.555ï 597, 2005.

4. He J. H., Lao C. S., Chen L . J., Davidovic D. and Wang Z. L. J. ñLarge-Scale Ni-Doped ZnO Nanowire Arrays and Electrical and Optical Propertiesò J. Am. Chem. Soc. Vol. 127, P. 16376-16377, 2005.

5. Hwang D. K,, Oh M. S., Lim J. H., and ParkJuan S.J, HaiAn S., Wei1 Z., et. al. ñZnO thin films and light-emitting diodesò Phys. D: Appl. Phys. Vol. 40, P. R 87ï R412, 2007.

6. Sathananthan S., Fan S.W., and Dravid V.P., ñHydrogen-Sensing Characteristics of Palladium-Doped Zinc-Oxide Nanostructuresò Nanoscape Vol. 6, Issue 1, 2009.

7. Zhou L., Gu P., and Zhou Y., ñPiezoelectric f ilm electro-deposition for optical f iber sensor with ZnO coatingò Chinese Optics Lett. Vol. 6, No. 6, 2008.

8. Wu D., Xu Q.Y., Zhang F.M., Liu X. S., Du Y. W., ñDiluted Magnetic Semiconductors and Spin Transport in Organic Materialsò AAPPS Bulletin, Vol. 18, No. 5, 2008.

9. Juan Y.X., HaiAn S., Wei Z., Hua X.U., ZaiXin Y., Tong A.C., & Wei1 D. U., ñRoom temperature ferromagnetism of Ni, (Ni, Li), (Ni, Ni doped ZnO thin filmsò Sci. China Tech Sci Vol.53, No.2 P. 293ï 296, 2010.

10. Pavle V., Radovanovic, and Daniel R., ñHigh-Temperature Ferromagnetism in Ni Doped ZnO Aggregates Prepared from Colloidal Diluted Magnetic Semiconductor Quantum Dotsò Phys. Rev. Lett. Vol. 91, No.15, P. 1-4, 2003.

11. Islam M. R., and Podder J., ñOptical Properties Of ZnO nano fiber thin films grows by spray pyrolysis of zince acetate precursorò Cryst. Res.Technol.Vol. 44, No.3, P. 286-292, 2009.

12. Nina V., Georgi G., Yordanov, Ceco D. and Dushkin, ñPhotocatalytic action of ZnO thin films prepared by the solï gel methodò React. Kinet Calat. Lett. Vol. 98 P. 259ï 263, 2009.

13. Huang X., Li G., Cao B., Wang M., and Hao C. ñMorphology Evolution and CL Property of Ni-Doped Zinc Oxide Nanostructures with Room-Temperature Ferromagnetismò J. Phys. Chem. C, Vol. 113, P. 4381ï 4385, 2009.

14. Elilarassi, R., Chandrasekaran, G., ñSynthesis, structural and optical characterization of Ni-doped ZnO nanoparticlesò J. Material Sci: Mater. Elec., DOI 10.1007/s10854-010-0206-8, 2010.

15. Liu X. J., Zhu X. Y., Song C., Zeng F., and Pan F., ñIntrinsic and extrinsic origins of room temperature ferromagnetism in Ni-doped ZnO filmsò J. Phys. D: Appl. Phys. Vol. 42 , P. 035004, 2009.

16. Zhang B., Zhang X. T., Gong H. C., Wu Z. H., Zhou S. M., and Liang D., ò Ni-doped Zinc Oxide nanocombs and phonon spectra propertiesò Phys. Lett. A. Vol. 372, P. 2300ï 2303, 2008.

17. Hwang D. K., Oh M. S., Lim J. H. and Park S. J. ñZnO thin films and light-emitting diodesò J. Appl. Phys. Vol. 40, P. 387ï 412, 2007.

18. Huang G. J., Wang J. B., Zhong X. L. Zhou G. C., and Yan H. L. ñSynthesis, structure, and room-temperature ferromagnetism of Ni doped ZnO nanoparticlesò J. Mater Sci. Vol. 42, P. 6464ï 6468, 2007.

CHAPTER –II

TECHNIQUES OF THIN FILM DEPOSITION & FILM FORMATION

CHAPTER –II

TECHNIQUES OF THIN FILM DEPOSITION & FILM FORMATION

A. Deposition Techniques of Thin Film

2.1 Introduction

Thin film can be prepared by various techniques, which are greatly influencing the physical properties of films. To know the property of metals, semiconductors and insulators create thin film on a substrate and measuring different properties.

2.2 Classification of deposition techniques

The different technique for producing thin film is given below.

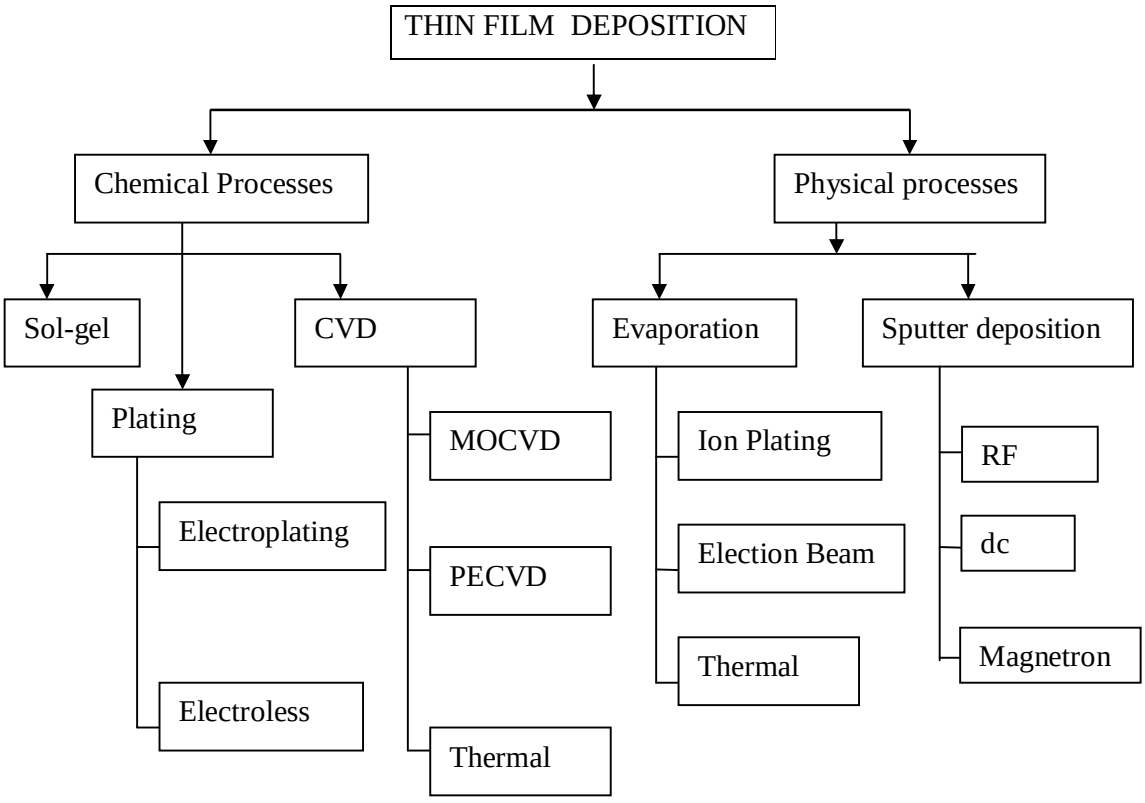

2.3 Some common deposition method

In this chapter some of the commonly used techniques are described briefly. But our aim is to prepare films by spray pyrolysis method, so spray pyrolysis method has been discussed below.

2.3.1 Thermal or vacuum evaporation method

The thermal evaporation is the simple, convenient and most widely used method for the preparation of thin films. In this method, materials are vaporized by heating it to a sufficient high temperature and the condensation of the vapor into a relatively cooler substrate yielding thin solid films [1].

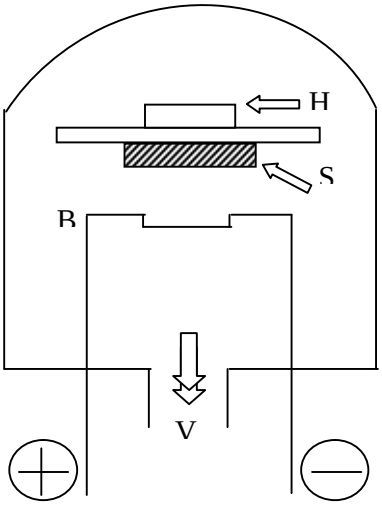

Fig. 2.1: Thermal vacuum evaporation.

Thermal evaporation may be performed directly or indirectly by variety of physical method. Several variants are

i) Resistive heating
ii) Exploding wire technique,
iii) Flash evaporation,
iv) Arc evaporation,
v) Laser evaporation,
vi) R.F. heating and
vii) Electron bombardment

2.3.2 Pulsed laser deposition

Pulsed laser deposition (PLD) is a thin film deposition technique where a high power pulsed laser beam is focused inside a vacuum chamber to evaporate material from

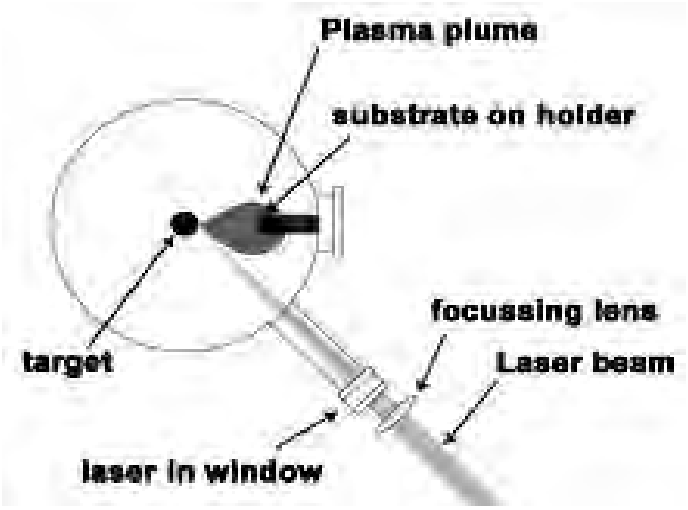

Fig: 2.2: Pulsed Laser Deposition (PLD)

a target of the desired composition and deposited as thin film on a substrate [2]. The laser pulse is absorbed by the target and energy is first converted to electronic excitation and later on into thermal, chemical and mechanical energy, which result in evaporation, ablation and plasma formation [3]. The ejected species expand into the surrounding vacuum in the form of a plume containing many energetic species including atoms, molecules, electrons, ions and particles, before depositing on the typically hot substrate.

2.3.3 Sputtering

Sputtering is a process whereby atoms are ejected from a solid target material due to bombardment of the target by energetic ions and is commonly used for thin-film deposition, etching and analytical techniques [4]. Sputter deposition is a method of depositing thin films by sputtering material from a target which is then deposited onto a substrate. Atoms can be ejected from the target by momentum exchange

between the sputtering ions and the target atoms, due to collisions. The average number of atoms ejected from the target per incident ion is called the sputter yield.

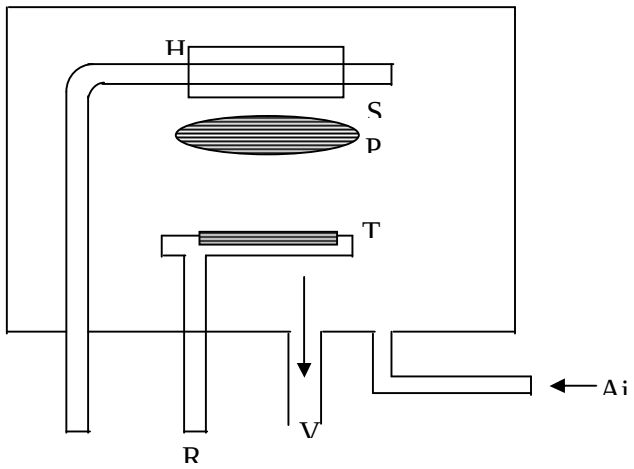

Fig. 2.3: Sputtering method.

The sputtering yield from the target is thereby one of the main parameters for sputter deposition of thin films and depends on the ion incident angle, the energy of the ion, the masses of the ion and target atoms, and the surface binding energy of atoms in the target. Sputtered atoms and ions ejected from the target have a wide energy distribution, whereas the sputtered ions can ballistically fly from the target in straight lines and impact energetically on the substrates or vacuum chamber (causing resputtering) [5]. However, the sputtered ions could also collide with gas atoms which act as moderator or as necessary growth reactant. Typically an inert gas is used for sputtering (for example argon or xenon).

2.3.4 Sol-gel process

The sol-gel process is a wet-chemical technique for the deposition of materials starting either from a chemical solution (sol for solution) or colloidal particles (sol for nano-scale particle) to produce an integrated network (gel) [6]. Sol-gel method is

a wet chemical route for the synthesis of colloidal dispersions of oxides which can be altered to powders, fibers, thin films and monoliths.

In general, sol-gel method consists of hydrolysis and condensation reactions. Sol-gel coating is a process of preparation of single or multicomponent oxide coating which may be glass, glass ceramic or crystalline ceramic depending on the process. Also, the nanomaterials used in modern ceramic and device technology require high purity and facilitate to control over composition and structure. The sol-gel coating is one of the interesting methods because it has many advantages [7-9]. Examples are as the followings

1. The chemical reactants for sol-gel process can be conveniently purified by distillation and crystallization.
2. All starting materials are mixed at the molecular level in the solution so that a high degree of homogeneity of films can be expected.
3. Organic or inorganic salts can be added to adjust the microstructure or to improve the structural, optical and electrical properties of oxide films.
4. The sol-gel coating is almost exclusively applied for fabrication of transparent layers with a high degree of planarity and surface quality.

2.3.5 Chemical vapor deposition (CVD) method

The deposition of films from gaseous phases by thermal decompositions or chemical reactions on substrate surfaces at high temperature is known as the chemical vapour deposition [10] process. This technique is used for the preparation of various inorganic as well as organic compounds. The basic principle involves decompositions or partial dissociations of the vapor phase species in a neutral atmosphere or otherwise and the deposition of the products. Sometimes a carrier gas is also introduced either to control the rate of reaction or to prevent undesired reactions at the prevailing elevated temperature.

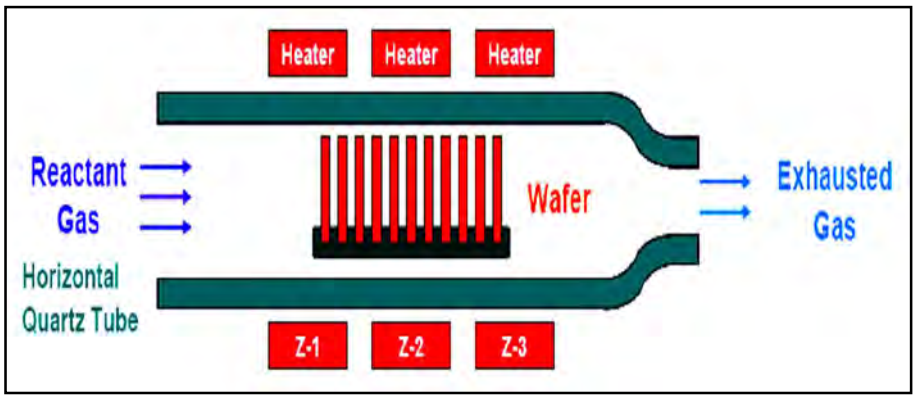

Fig.2.4: Chemical Vapor Deposition (CVD)

An appropriate control of the rate of flow of the gaseous species, temperature and pressure of the reaction chamber leads to the formation of required deposits.

2.3.6 Spin coating

Spin coating has been used for several decades for the application of thin films. It is a procedure used to apply uniform thin films to flat substrates Spin Coating involves the acceleration of a liquid puddle on a rotating substrate [11].

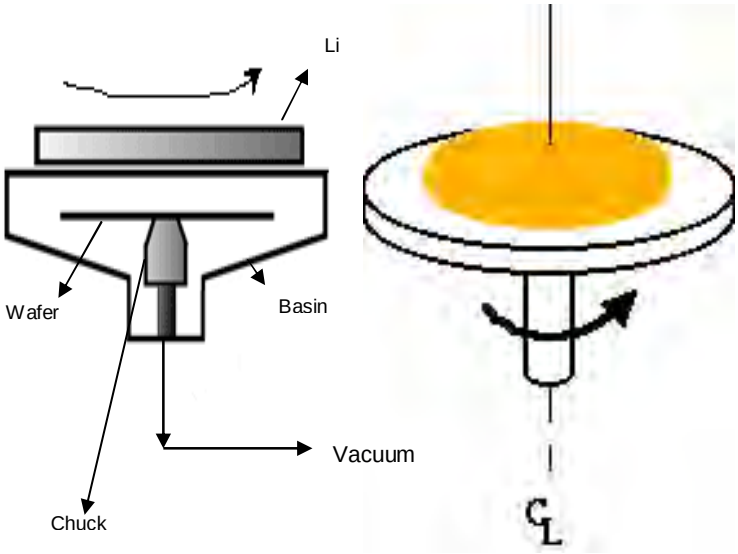

Fig. 2.5: Spin Coating

A typical process involves depositing a small puddle of a fluid resin onto the center of the substrate and then spinning the substrate at high speed. The film-forming process is primarily driven by two independent parameters ï viscosity and spin speed. The range of film thicknesses easily achieved by spin coating is 1-200 m m. For thicker films, high material viscosity, low spin speed, and a short spin time are needed. However, these parameters can affect the uniformity of the coat. Multiple coatings are preferred for a film thickness greater than 15mm.

2.3.7 Spray pyrolysis method

Spray pyrolysis is a powerful technique to synthesize a wide variety of high purity chemically homogeneous ceramic powders [12]. Large quantities of oxide powders with homogeneous particle sizes and crystalline sizes less than 100 nanometers may be produced by this method. This is one of the best methods for the deposition of thin films.

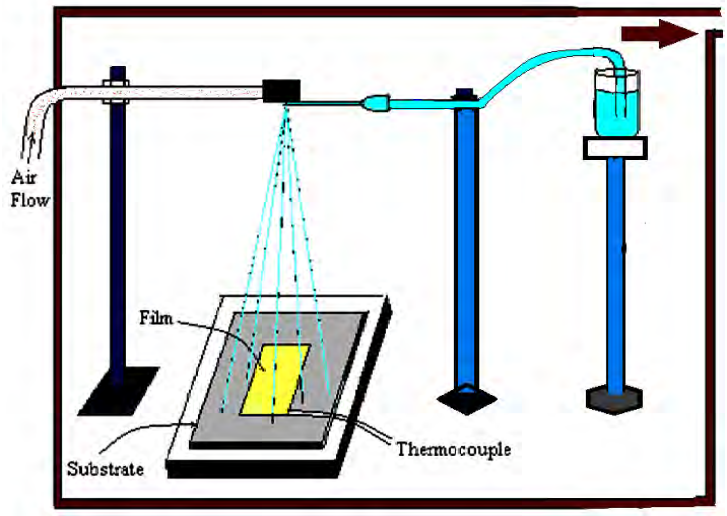

Fig. 2.6 : Spray Pyrolysis Method

The method involves spraying a solution usually in aqueous, containing soluble of the constituent atoms of the desired compound on to a heated substrate. Every sprayed droplet reaching the substrate undergoes pyrolysis decomposition and forms a single crystallite or a cluster of crystallites of the products. Different parameter like

volume of solution sprayed substrate temperature, solution and flow rates concentration of the solution distance between the substrate and the spray nozzle have to be optimized to get a homogeneous uniform thickness and good quality of the film. Hydrolysis and pyrolysis are the main chemical reactions involved in this process. In this technique, the chemicals vaporized and react on the substrate surface after reaching on it. In principle spray pyrolysis technique is very simple, cost effective and suitable for industrial applications [13]. The apparatus, needed to carry out the chemical spray process, consists of an atomizer the spray solution and a substrate heater. The spray deposition has been used to prepare coatings for the cover glass, required for flat plate collectors and cutter tubes used in the focusing type cylindrical collectors.

B. FILM FORMATION

2.4 Introduction

Thin film is prepared by deposition of the film materials (metals, semi-conductors, insulators, dielectric etc.) atom by atom on a substrate through a phase transformation. Sufficient time interval between the two successive deposition of atoms and also layers are required so that these can occupy the minimum potential energy configuration. In thermodynamically stable films, all atoms or molecules should be in their minimum potential energy sites and incoming atoms or molecules will take up positions and orientations energetically compatible with the neighboring atoms of the substrate or to the previously deposited layers, the effect of substrate or the initial layers will diminish gradually [14].

2.4.1 Different stages of film formation

There are three mechanism of thin film condensation which can be distinguished, depending on the strength of interaction between the atoms of the growing film and between the atoms of the film and substrate. These are

In the **Frank-van der Merwe** or **layer-by-layer** growth mode, the **adsorbate-substrate** interaction dominates the **adsorbate-adsorbate** interaction and thus a new layer begins to grow only when the previous layer is completed.

i. In the **Vollmer-Weber** or **island** growth mode, the **adsorbate-adsorbate** interaction dominates and thus deposition produces multilayer islands.

ii. The **Stranski-Krastanov** or **layer+island** growth mode is a particularly interesting case that has recently been exploited in the production of nanometre scale islands. After the formation of 1 or more complete monolayers, three dimensional islands nucleate and grow on top of the complete layer.

In most cases, mechanism (ii) takes place and we shall focus our attention on this mechanism in brief.

2.4.2 Condensation

Thin films are most commonly prepared by the condensation of atoms on a substrate from the vapor phase of the material. Condensation means the transformation of a gas in to a liquid or solid. Thermodynamically, the only requirement for

condensation to occur is that partial pressure of the film material in the gas phase be equal or larger than its vapor pressure in the condensed phase at that temperature. Condensation of a vapor atom is determined by its interaction with the impinged surface. The impinging atom is attracted to the surface by the instantaneous dipole and quadruple moments of the surface atoms. Consequently the atoms losses its velocity component normal to its surface in a short time, provided the incident kinetic energy is not too high. The vapor atom is then physically absorbed (called ad atom) but it may or may not be completely thermally equilibrated [15]. It may move over the surface by jumping from one potential to the other because of the thermal activation from the surface and its own kinetic energy parallel to the surface. The ad atom has a finite stay or residence time on the substrate during which it may interact with other ad atoms to form stable cluster and be chemically absorbed with the release of the heat of condensation. If is not absorbed the ad atom re-evaporates or desorbs into the vapor phase. Therefore, condensation is the net result of equilibrium between the absorption and desertion process.

The probability that an impinging atom will be incorporated into the substrate is called the ñcondensationò or ñstriking coefficientò. It is measured by the ratio of the amount of material condensed on a surface to the total amount impinged. In fact, often the striking coefficient is so small that condensation is not observable by ordinary techniques. On the other hand, the striking coefficient is found to be strongly dependent on the total time during which the substrate was subjected to the impingement, and also on the substrate temperature. A non- unity striking coefficient is usually explained in terms of monomer re-evaporation form the areas on the substrate, which are outside, the capture zones around each stable nucleus [16].

2.4.3 Nucleation

Nucleation is the birth stage of a film. Condensation is initiated by the formation of small cluster through the combination of several absorbed atoms. These clusters are called nuclei and the process of formation is called nucleation.

There are two types of nucleation occur during the formation of a film. They are

a) **Homogeneous nucleation:** The total free energy is used in the formation of a cluster of ad-atoms.
b) **Heterogeneous nucleation:** Particular shapes of clusters are formed by collisions of atoms on the substrate surface, and in the vapor phase its super saturation is sufficiently high. They initially developed within increase in free energy until a critical size is reached above which growth continues with a decrease in free energy. In atomistic theory, in low substrate temperature or very high super saturations, the critical nucleus may be a single atom which will form a pair with another atom by random occurrence to become a stable cluster and grow spontaneously.

2.4.4 Growth

There are several stages in the growth process from the initial nucleation of the deposits to the final continuous three dimensional film formation states. These stages of film growth have been observed by many workers from their electron microscopic and other studies. These are valid not only for deposits condensing from the vapor phase but also for others, i.e. for solutions, by electro deposition, chemical reactions anodic oxidation, etc. There are four stages of the growth process based on the electron microscope observations [17]. They are

(i) The island stage/Nucleation growth stage
(ii) The coalescence stage
(iii) The continuous film stage

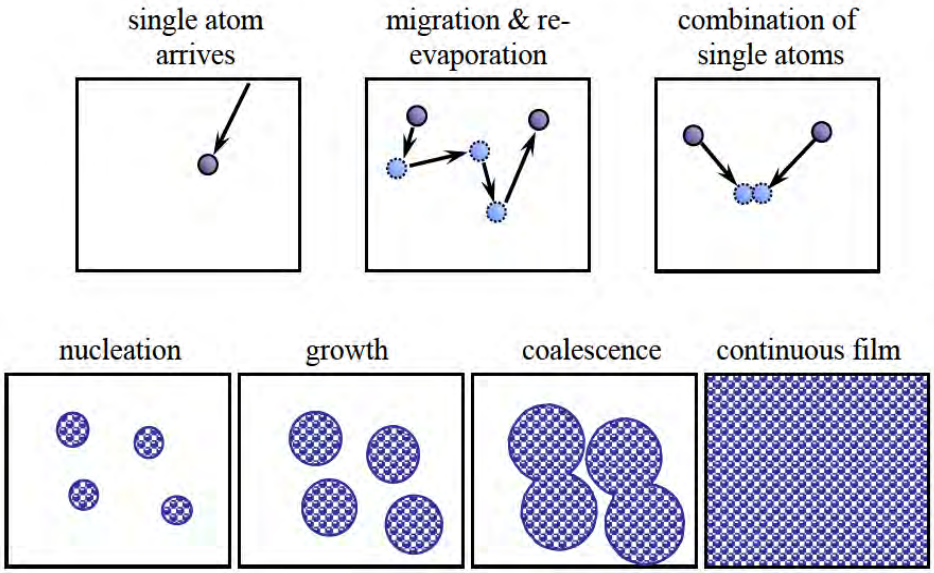

Fig.2.7: The stages of the film growth.

2.4.5 The island stage

When a substrate under impingement of condenses monomers is observed in the electron microscope, the first evidence of condensation is a sudden burst of nuclei of fairly uniform size. The smallest nuclei detected have a size of 2.0 to 3.0 mm. Growth of nuclei is three dimensional, but the growth parallel to the substrate is greater than that normal to it. This is probably because growth occurs largely by the surface diffusion of monomers on the substrate, rather by direct impingement from the vapor phase. The tendency to form an island structure is increased by (a) at high substrate temperature, (b) at low boiling point film material, (c) at low deposition rate, (d) at weak binding energy between film material and substrate, (e) at high surface energy of the film material and (f) at low surface energy of the substrate.

2.4.6 The Coalescence stage

As island increases their size by further deposition and come closer to each other, the larger ones appear to grow by coalescence of the smaller ones. The coalescence occurs in less than 0.ls for the small nuclei. In addition, nuclei having well-defined crystallographic shapes [18] before coalescence become rounded during the event. The composite island takes on a crystallographic shape again if left for a sufficiently long time before interacting with its neighbors.

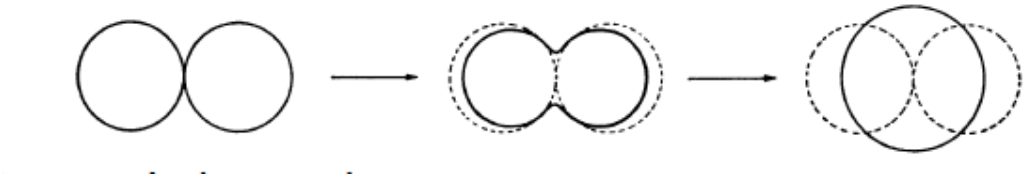

Fig.2.8: Coalescence of two supercritical nuclei and Shape change during coalescence.

2.4.7 The continuous film stage

It is the final stage of the film growth. This process is slow and filling the empty channels which requires a considerable amount of deposits. These empty channels are filled by secondary nucleation, growth and coalescence and in this way of a continuous film are formed.

2.5 Characteristics of thin films

The properties of thin film changes appreciably when it is cooled to a very low temperature or heated at a higher temperature (above room temperature). The study of the changes in the properties of thin film with temperature provides a great deal of information about the properties of thin films. In general the physical properties of thin film are determined by a number of factors, such as

i) The nature of substrates

It may be non-crystalline solids e.g., glass of vitreous silica or crystalline such as cleavage plates of rock salt or mica. To select a particular substrate one has to take into consideration of the lattice parameter of the substrate so that it matches to the lattice parameter of the grown film, otherwise structural mismatch may create mechanical fracture in the film. It is also necessary to consider the melting point of the substrate material. It should be comparable with that of the film materials.

ii) Substrate temperature

The temperature of substrate during deposition of film may affect the film properties. At low temperature polycrystalline films with high densities of structural imperfections are formed on both vitreous and crystalline substrate, but a high temperature oriented single crystal films are formed on crystalline substrates.

iii) Deposition rate and film thickness

The temperature at which epitaxy occurs is dependent on the deposition rate. Substrate temperature decreases with increasing deposition rate. Film thickness mainly depends on deposition rate and deposition time. If the deposition rate increases, the film thickness also increases having the same deposition time.

iv) Post-deposition annealing of the films

Heating the film to a higher temperature after deposition and cooling it back to room temperature is known as annealing. Properties of the deposited films are related to the annealing temperature. The post-annealing process removes some defects of the films. It plays an important role in the surface mobility of the atoms.

Reference

1. Thota S., Dutta T., and Kumar J., ñOn the solï gel synthesis and thermal, structural, andmagnetic studies of transition metal (Ni, Co, Mn) containing ZnO powdersò J. Phys. Condens. Matter, Vol. 18, P. 2473ï 2486, 2006.

2. Singh S., Nakamura D., Sakai k., Okada T., and Rao M. S. R., ñInvestigation of low-temperature excitonic and defect emission from Ni-doped ZnO nanoneedles and V-doped ZnO nanostructured filmò New J. of Phys. Vol. 12, P. 023007 (11p), 2010.

3. Pearton S.J., David P., Matt P., Hebard F., etl. ñZnO Doped With Transition Metal Ionsò IEEE Trans. on Electron Dev., Vol. 54, NO. 5, 2007.

4. Pandey B., Ghosh S., Srivastava P., Kabiraj D., Shripati T. and Lalla N. P., ñSynthesis of nano dimensional ZnO and Ni-doped ZnO thin films by atom beam sputtering and study of their physical propertiesò J. Phys. Vol. 41, Issue 7, P. 1164-1168, 2009.

5. Chopra K. L., ñNucleation, Growth and Structure of Filmsò Thin Film Phenomena, McGraw-Hill Book Company-New York, P. 110-137, 1969.

6. Gaewdang N., Gaewdang T., and Lipar W., ñSome Characterization of Chemical Bath Co-Deposited CdS-ZnS Thin Filmsò Tech. Digest of the inter. PVSEC, Vol-14, P. 583-584, 2004.

7. Xiao H., Xianogyan Z., Uddin A. and Leu C. B., ñPreparation and characterization of electronic and optical properties of plasma polymerized nitritesõõ, Thin Solid Films, Vol-477, P. 81-87, 2005.

8 Ilican, Caglar M. and Caglar Y., ñThe effect of deposition parameters on the physical properties of $Cd_xZn_{1-x}S$ films deposited by spray pyrolysis methodõõ, J. of Opt. and Adv. Mater., Vol-9, P. 1414-1417, 2007.

9. Elilarassi R., and Chandrasekaran G., ñSynthesis and optical properties of Ni-doped zinc oxide nanoparticles for optoelectronic applicationsò Optoelectron. Lett. Vol.6 No.1, 2010.

10. Pan M., Rondon R., Cloud J., Rengarajan V., Nemeth W., Valencia A., Gomez J., Spencer N., Nause J., ñZnO Based Light Emitting Diodes Growth and Fabricationò Proc. of SPIE Vol. 6122 61220.

11. Dana A., Schwartz, Kevin R., Kittilstved and Daniel R., ñAbove-room-temperature ferromagnetic Ni2+-doped ZnO thin films prepared from colloidal diluted magnetic semiconductor quantum dotsò Appl. Phys. Lett., Vol.85, 2004.

12. Kalyana C., Pingali, Deng S., and David A. Rockstraw ñSynthesis of Nanowires by Spray Pyrolysisò J. of Sensor. Vol.6, ID 683280, 2009.

13. Raviprakash Y , Kasturi V. B, Shivakumar G.K. ñPreparation and characterization of CdxZn1-xS thin films by spray pyrolysis technique for photovoltaic applicationsò J. Phys. Condens. Matter Vol.83, P.1645ï 1651, 2009.

14. Lampkin, Curt M., ñAerodynamics of nozzles used in spray pyrolysisò, Prog. Crys. Growth. P. 406-416, 1979.

15. Pavlo I. Stakhira, L. Georgij, Pakhomov V. Vlad, Cherpak, ñPhotovoltaic cells based on nickel phthalocyanine and zinc oxide formed by atomic layer depositionò Cent. Eur. J. Phys. Vol. 8, P. 798-803, 2010.

16. Chopra, K. L., óóNucleation, Growth and Structure of Filmsò Thin Film Phenomena, McGraw-Hill book Company, New York, P. 110-137, 1969.

17. Jensen, P. Havlin, S. et al. ñA Fractal Model for the first stage of thin films growthò Fractals, Vol. 4, No. 3, P. 321-329, 1996.

18. Ratsch, C., Venables, J. A. ñNucleation theory and the early stages of thin film growthò J. Vacuum. Sci. Techn. P. 0734-2101, 2003.

CHAPTER- III

EXPERIMENTAL DETAILS

CHAPTER- III
EXPERIMENTAL DETAILS

3.1 Introduction

This chapter deals with mainly the design and construction of different experimental apparatuses and preparation of $Zn_{1-x}Ni_xO$ thin films on glass substrate. Various steps taken for the film on glass substrate by spray pyrolysis deposition process will be discussed in the latter part of this chapter. Spray pyrolysis is the most commonly used technique adopted for the deposition of metals, alloys and many compounds [1] Processes involved in spray pyrolysis technique, such as atomization of the precursor solution, aerosol transport, and decomposition of the precursor are discussed in this chapter.

3.2 Experimental Equipment

3.2.1 Preparation of Mask

In order to study the various properties of thin film, it is necessary that they must be properly patterned. The most commonly used method of patterning thin film is the physical masking, which is accomplished by placing the mask of desired shape on the substrate. We found mica and stainless steel as suitable masking material. Since the thickness of the films deposited is of the order the mask should be as thin as possible so as to obtain uniformity of thickness throughout the film pattern.

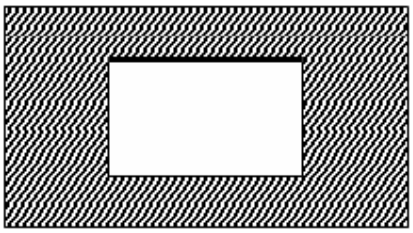

Fig. 3.1: Mask used for the preparation of films

3.2.2 Experimental setup of spray pyrolysis technique

The design of a typical reactor is shown in Fig. (3.2). It is a vertical batch type reactor composed of a galvanized iron enclosure , heater , and heat susceptor . For the rapid expulsion of the byproduct gasses there are opening at the side and at the top of the reactor. It helps focusing the incoming aerosol towards the substrate and also provides a chimney action to the exhaust gas upwards.

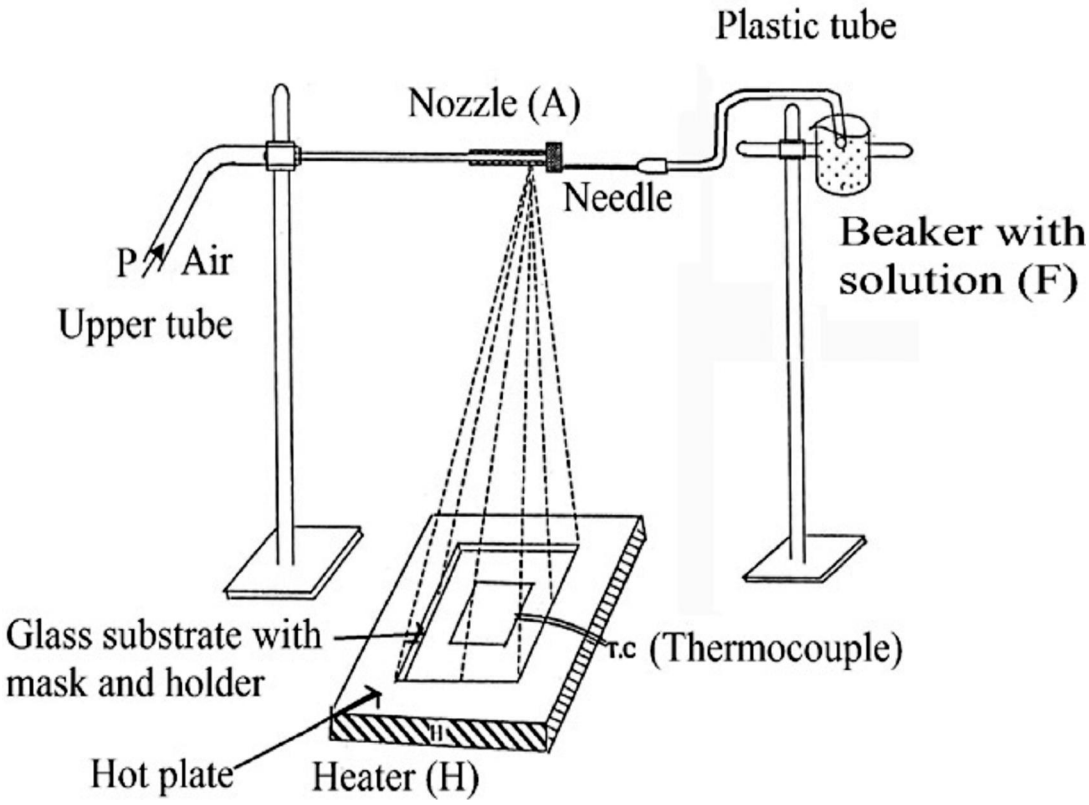

Fig.: 3.2: Experimental setup of Spray Pyrolysis technique.

3.2.3 Heater

The heater óHô is an ordinary hot plate 2-kilowatt nichrome wire heater. The top of the plate is covered with a thick sheet of stainless steel plate. Substrate is placed on this plate to have a uniform temperature throughout the substrate surface. A mica sheet with the same design of mask is placed in between the substrate and the mask to prevent spreading in solution beyond the opening of the mask. An electrical voltage variac controls the heater power. The temperature of the heater was measured by copper constantan thermocouple tightly attached to the substrate surface placed on the heater susceptor.

3.2.4 Air Compressor

It is a reservoir type electrical air compressor. A rotary pump in this section mode draws atmospheric air and keeps it reverse in a large capacity air tank. At the outlet of the tank a pressure gauge is attached which records the pressure of the air at the time of supplying it from the tank. There is a bypass control valve which can keep the output pressure constant.

3.2.5 Head/ Nozzle

The single spray nozzle consists of capillary tubes (stainless steel) fitted at perpendicular to the other tube as shown in Fig.3.2. When compressed air is passed rapidly through the upper tube óPô in direction tangential to the mouth of the lower tube óAô whose other end is kept deep in the spray liquid. Due to this partial vacuum the liquid rises up through the tube óAô and the compressed air drives it away in the form of the fine spray particles (aerosol). The thinner the spray nozzle the finer would be the spray particles. A very fine needle shaped capillary tube was used for the spray nozzle.

3.2.6 The fume chamber

It is a large box type chamber with a slanting top and is provided with a chimney. There is an exhaust fan with regulated power supply fitted at the top of the chimney [3]. The slanting top and the sidewalls are made of glass. There are air tight doors in the front side. The chamber has purging facilities. The whole spray system is kept inside the fume chamber at the time of film deposition because of Safety grounds and to check air current disturbances at the deposition site. These two points just stated are very important for the pyrosol process when deposition is carried out in open air atmosphere.

3.2.7 Substrate and substrate cleaning

The most commonly available microscope glass slides were used as substrates in the present work. The cleanliness of substrate surface exerts a decisive influence on film growth and adhesion. A thoroughly cleaned substrate is a pre-requisite for the preparation of films with reproducible properties. The choice of cleaning techniques depends on the nature of the substrate, the type of contaminants and the degree of cleanliness required. Since our glass substrates were ordinary soda lime microscope slides and over slides and therefore residue from manufacturing and packaging, fingerprints, oils and air borne particulate maters were supposed to be contaminations. The following procedure was found adequate for substrate cleaning in our laboratory. The gross contaminations of each of the substrates are first removed by warm aqueous solution of sodium carbonate.

After washing in a stream of cold water they are dipped at first into nitric acid for some time and then washed in de-ionized water several times and finally made dry by blowing hot air [4]. They are then preserved in desiccators. During the whole process slide, holding forceps always held the substrates.

3.2.8 Solution preparation

The solution was prepared by taking Zn $(CH_3.COO)_2.2H_2O$ as source compound. The most commonly used solvents are water. As Ni $(CH_3.COO)_3.4H_2O$ dissolves in water at room temperature, water was taken as solvent. Since the spray system used

in the present experiments operates via a partial vacuum path at the mouth of the spray nozzle, the concentration of the solution prepared by the solvent should be such that the nozzle could at least draw it. The higher the solution concentration, the lower the spray rates.

$$\left.\begin{matrix} Zn(CH_3COO)_2.2H_2O \\ + \\ Ni(CH_3COO)_3.4H_2O \end{matrix}\right\} \xrightarrow{300^\circ C} Zn_{1-x}Ni_xO\downarrow + CO_2\uparrow + CH_4\uparrow + Steam\uparrow$$

Nickel was added in the form of nickel acetate in the working liquid. In this work, 1%, 3%, 5%, 10%, 15% and 20% (wt%) of Nickel was used for the purpose of doping.

3.2.9 Rate of deposition

The rate of flow of the working solution can be controlled to a better accuracy by suitably designing the nozzle A and adjusting the air flow rate. In preparing ZnO films, the solution flow rate of 0.5ml/min to 0.7ml /min was used for the present experiment.

3.2.10 Film thickness and control

Thickness plays an important role in the film properties unlike a bulk material and almost all film properties are thickness dependent at least for thin films. Reproducible properties are achieved only when the film thickness and the deposition parameters are kept constant [5-7].

In the present spray deposition process, the deposition time is the main thickness-controlling factor, provided the other parameters remain constant. Since the deposition is carried out in normal atmosphere a direct control of thickness is not so easy. To control the film thickness therefore calibration chart may be used. The charts are generally plots of deposition time versus thickness, and can be prepared at different constant substrates temperatures prior to the preparation of particular

experimental samples using the different solution and deposition variables. Since the rate of deposition in present set up is rather small, the thickness control is therefore not difficult.

3.3 Steps of thin film processes

There are four sequential steps are followed when a thin film is growth on a substrate. A source of film material is provided, the material is transported to the substrate, deposition take place, so the film is subsequently annealed, and finally it is analyzed to evaluate the process. The results of the analysis are then used to adjust the condition of the steps for film property modification.

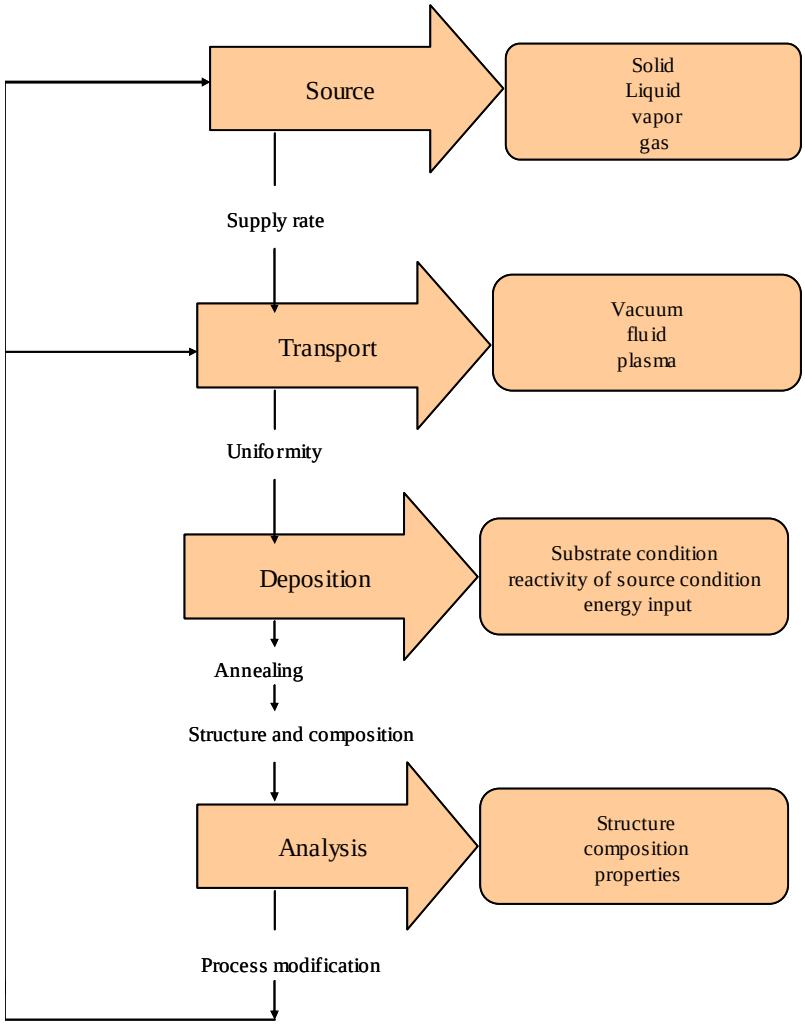

Fig. 3.3: Thin films process

3.4 Sample deposition

It has been declared earlier that spray pyrolysis method for preparing thin films is an economically attractive method [8-10], which consist basically of spraying solution on a heated glass substrate. The apparatus needed to carry out the chemical spray process consists of a device to atomize the spray solution and a substrate heater. Figure 3.2 shows a typical experimental setup. A considerable amount of 100 ml solution taken in the container óFô fitted with the spray nozzle óAô. The clean substrate with a suitable mask was put on the heater óHô. The distance between the tip of the nozzle and the surface of the glass substrate was kept 25 cm. Before supplying the compressed air the substrate temperature óT_sô was to be kept at a level slightly higher than the required substrate temperature because at the onset of spraying a slight fall of temperature is likely. The temperature of a substrate was controlled by controlling the heater power using a variac. The substrate temperature was measured by placing a copper constant thermocouple on the substrate. When compressed air is passed through óPô at constant pressure (0.5 bar), a fine $Zn_{1-x}Ni_xO$ was produced and was automatically carried to the reactor zone where film was deposited on the heated substrate [11-12].

References

1. Antonaia P., Menna, M. L., Addonzio, and Crocchilo, ñTransparent properties of polycrystalline tin oxide filmsò Sol. Energy Mater, Vol. 28, P. 167-173.

2. Mohammad T.M., ñPerformance and characteristics of L-PbS/SnO_2: F selective coating system for photothermal energy conversionò Sol. Energy Mater, Vol. 20, P. 297-305, 1990.

3. Patil P. S., Kadam L. D., Lokhande C. D.,ñPreparation and characterization of spray pyrolysed cobalt oxide thin filmsò Thin Solid Films, Vol. 272, P. 29-32, 1996.

4. Choudhury C., and Sehgal H. K., ñProperties of Spray deposited Cobalt Oxide Selective Coating on Aluminium and Galvanised Iron Substrateò Appl. Energy, Vol. 10, P. 313-324, 1982.

5. Kadam L. D., Patil P. S., ñThickness-Dependent Properties of Sprayed Cobalt Oxide Thin Filmsò Mater. Chem. and Phys., Vol. 68, P. 225ï 232, 2001.

6. Kadam L. D., Pawar S. H., and Patil P.S., ñStudies on ionic intercalation properties of cobalt oxide thin films prepared by spray pyrolysis techniqueò Materials Science Communication, Mater. Chem. and Phys. Vol. 68, P. 280ï 282, 2001.

7. Korotcenkov G., Brinzari V., Boris I., ñ(Cu, Fe, Co, or Ni)-doped tindioxide films deposited by spray pyrolysis: doping influence on film morphologyò J. Mater. Sci., 43, p. 2761ï 2770, 2008.

8. Jachon J., Varghes M., and Abraham K. E., ñStudies on Cu, Fe, and Mn Doped SnO_2 Sem Conducting Transparent Films Prepared by a Vapor Deposition Techniqueò Chines. J. of Phys., Vol. 45, No.1, P. 84-97, 2007.

9. Hong N. H., Sakai J., Prellier W., Hassini A., ñTransparent Cr-doped SnO_2 thin films ferromagnetism beyond room temperature with a giant magnetic momentò J. Phys. Condens. Matter., Vol. 17, P. 1697ï 1702, 2005.

10. Korotcenkov G., Macsanov V., Tolstoy V., Brinzari V., Schwank J. and Faglia G., ñStructural and gas response characterization of nano-size SnO_2 films deposited by SILD methodò, Sensor. and Actu. B: Chem., Vol. 96, 3, P. 602-609, 2003.
11. Anuar K., Ho S. N., Tan W. T., Atan M. S., Kuang D., Jelas H. M., Saravanan N., ñEffects of Solution Concentration on the Properties of Cu_4SnS_4 Thin Filmsò Mater. Sci., Vol.14, No.2, 2008.

12. Elangovan E., Ramamurthi K, ñStudies on optical properties of polycrystalline SnO_2:Sb thin films prepared using $SnCl_2$ precursorò Cryst. Res. Technol., Vol.38, No. 9, P. 779-784, 2003.

CHAPTER-IV

THEORETICAL BACKGROUND OF THIN FILM

CHAPTER-IV

THEORETICAL BACKGROUND OF THIN FILM

4.1 Introduction

The optimization of the preparation conditions is the main task in order to get device quality films. This is to be done on the basis of detailed structural, compositional, morphological, optical and electrical properties of the films obtained at different growth conditions. In the following sections the techniques used for the film characterizations are discussed briefly.

4.2 Scanning electron microscopy (SEM) study

The surface morphology of the films was taken by scanning electron microscope (SEM). The scanning electron microscope (SEM) is a type of electron microscope that images the sample surface by scanning it with a high-energy beam of electrons in a raster scan pattern [1]. There are many advantages to using the SEM instead of a light microscope. The SEM has a large depth of field, which allows a large amount of the sample to be in focus at one time. The SEM also produces images of high resolution, which means that closely spaced features can be examined at a high magnification [2]. A beam of electrons is generated in the electron gun, located at the top of the column, which is pictured to the left. This beam is attracted through the anode, condensed by a condenser lens, and focused as a very fine point on the sample by the objective lens. The scan coils are energized (by varying the voltage produced by the scan generator) and create a magnetic field which deflects the beam back and forth in a controlled pattern.

The varying voltage is also applied to the coils around the neck of the Cathode-ray tube (CRT)

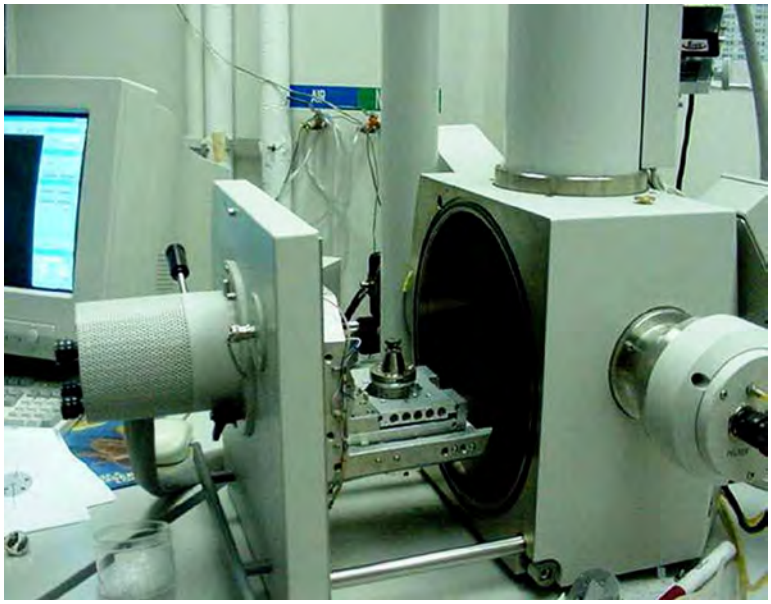

Fig. 4.1 : SEM microscope

This produces a pattern of light deflected back and forth on the surface of the CRT. The pattern of deflection of the electron beam is the same as the pattern of deflection of the spot of light on the CRT. The electron beam hits the sample, producing secondary electrons from the sample. These electrons are collected by a secondary detector or a backscatter detector, converted to a voltage, and amplified. The amplified voltage is applied to the grid of the CRT and causes the intensity of the spot of light to change. The image consists of thousands of spots of varying intensity on the face of a CRT that correspond to the topography of the sample.

The SEM column can be broken down into several component parts;

- An electron gun which provides a source of electrons.
- A pair of electromagnetic condenser lenses which produce a beam with a very small diameter.

- An objective lens to focus the beam on the specimen surface and scan coils to cause the beam to traverse across the specimen.
- The specimen chamber containing a manipulative stage and secondary electron detector.
- A vacuum system to remove the air from the electron optical column thus providing a free path for the beam electrons.

4.3 Compositional study

EDX Analysis stands for Energy Dispersive X-ray analysis. It is sometimes referred to also as EDS or EDAX analysis. It is a technique used for identifying the elemental composition of the specimen. The EDX analysis system works as an integrated feature of a scanning electron microscope (SEM), and can not operate on its own without the latter.During EDX Analysis, the specimen is bombarded with an electron beam inside the scanning electron microscope. The bombarding electrons collide with the specimen atoms' own electrons, knocking some of them off in the process. A position vacated by an ejected inner shell electron is eventually occupied by a higher-energy electron from an outer shell [3] To be able to do so, however, the transferring outer electron must give up some of its energy by emitting an X-ray. The amount of energy released by the transferring electron depends on which shell it is transferring from, as well as which shell it is transferring to. Furthermore, the atom of every element releases X-rays with unique amounts of energy during the transferring process. Thus, by measuring the amounts of energy present in the X-rays being released by a specimen during electron beam bombardment, the identity of the atom from which the X-ray was emitted can be established.

The output of an EDX analysis is an EDX spectrum. The EDX spectrum is just a plot of how frequently an X-ray is received for each energy level. An EDX spectrum normally displays peaks corresponding to the energy levels for which the most X-rays had been received [4]. Each of these peaks are unique to an atom, and therefore corresponds to a single element. The higher a peak in a spectrum, the more concentrated the element is in the specimen.

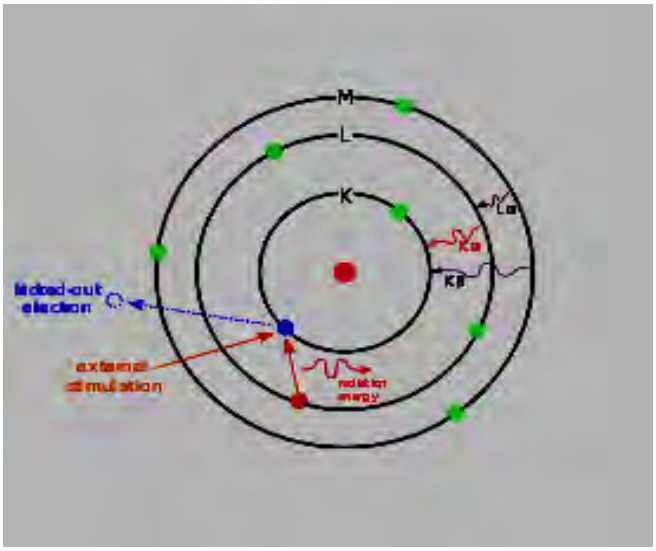

Fig. 4.2: Scheme of X-Ray excitations

An EDX spectrum plot not only identifies the element corresponding to each of its peaks, but the type of X-ray to which it corresponds as well. For example, a peak corresponding to the amount of energy possessed by X-rays emitted by an electron in the L-shell going down to the K-shell is identified as a K-Alpha peak. The peak corresponding to X-rays emitted by M-shell electrons going to the K-shell is identified as a K-Beta peak.

4.3 Structural analysis of thin films

Structural analysis of thin films is done by the X-ray diffraction (XRD) study. It is one of the oldest and effective tools for the determination of the atomic arrangement in a crystal. XRD is a very important parameter because it gives information about the phases of the films, it can give the identification of materials deposited on the film and can make differences between crystalline and amorphous materials. X-ray powder diffraction (XRD) is a rapid analytical technique primarily used for phase identification of a crystalline material and can provide information on unit cell dimensions. The analyzed material is finely ground, homogenized, and average bulk composition is determined.

4.4.1 X-ray diffraction (XRD) study

The X-ray diffraction (XRD) study provides substantial information on the crystal structure. X-rays are electromagnetic radiation of wavelength about 1 Å (10-10 m), which is about the same size as an atom. They occur in that portion of the electromagnetic spectrum between gamma-rays and the ultraviolet. The discovery of X-rays in 1895 enabled scientists to probe crystalline structure at the atomic level. X-ray diffraction has been in use in two main areas, for the fingerprint characterization of crystalline materials and the determination of their structure [5]. Each crystalline solid has its unique characteristic X-ray powder pattern which may be used as a "fingerprint" for its identification. Once the material has been identified, X-ray crystallography may be used to determine its structure, i.e. how the atoms pack together in the crystalline state and what the interatomic distance and angle are etc. X-ray diffraction is one of the most important characterization tools used in solid state chemistry and materials science. We can determine the size and the shape of the unit cell for any compound most easily using the diffraction of x-rays between two waves. When X-rays are incident on a crystal surface, they are reflected from it. The reflection obeys the following Braggôs law

$$2d_{hkl} \sin\theta = n\lambda \qquad 4.1$$

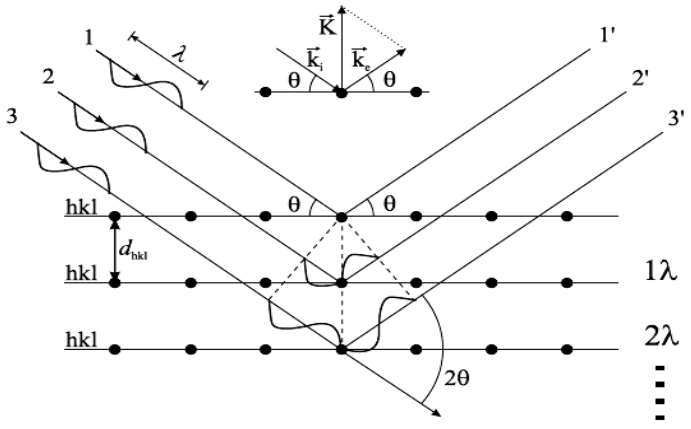

Fig. 4.3 : Reflection of x-rays from two planes of atoms in a solid.

Where d is the distance between crystal planes, ɗ is the incident angle of the X-ray, ə is the wavelength of the X-ray and n is a positive integer. Braggôs law also suggests that the diffraction is only possible when ə < 2d.

From the width of the diffraction line, it is possible to estimate the average grain size in the film [6]. The X-ray line broadening is commonly used to determine the crystallite size, which is given by

$$Dg = 0.9ə/qcosɗ \qquad 4.2$$

Where Dg is the average grain size, ə is the wavelength of the radiation used as the primary beam of Co KŬ (ə= 1.79012 Å), ɗ is the angle of incidence in degree and q is the full width at half maximum (FWHM) of the peak in radian. The dimensionless shape factor has a typical value of about 0.9, but varies with the actual shape of the crystallite [7].

4.4 UV-VIS spectroscopy

Ultraviolet (UV) and Visible (VIS) light can cause electronic transitions. When a molecule absorbs UV-VIS radiation, the absorbed energy excites an electron into an higher energy orbital. Ultraviolet radiation has wavelengths of 200-400 nm. Visible light has wavelengths of 400-800 nm.

Wavelength Region (nm)

Far ultraviolet 10-200

Near ultraviolet 200-400

Visible 400-800

Near infrared 800-3000

Middle infrared 3000-30,000

Far infrared 30,000-300,000

Microwave 300,000-1,000,000,000

A diagram (4.4) of the components of a typical spectrometer is shown in the following diagram. The functioning of this instrument is relatively straightforward.

A beam of light from a visible and UV light source (colored red) is separated into its component wavelengths by a prism or diffraction grating.

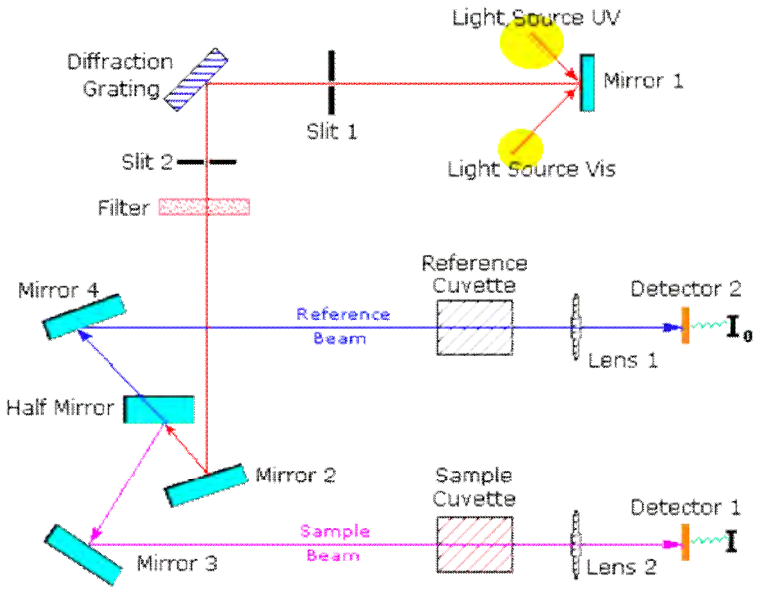

Fig. 4.4 : The components of a typical spectrometer

Each monochromatic (single wavelength) beam in turn is split into two equal intensity beams by a half-mirrored device. One beam, the sample beam (colored magenta), passes through a small transparent container (cuvette) containing a solution of the compound being studied in a transparent solvent. The other beam, the reference (colored blue), passes through an identical cuvette containing only the solvent. The intensities of these light beams are then measured by electronic detectors and compared. The intensity of the reference beam, which should have suffered little or no light absorption, is defined as $\mathbf{I_0}$. The intensity of the sample beam is defined as **I**.

4.6 Optical characterization of thin films

Optical properties of films have been studied extensively primarily because of their applications in various optical and electro-optical devices. The optical study of a solid concerns not only with the physical phenomena such as reflection, refraction,

transmission, absorption, polarization, interference of light but also the interactions of photon energy with matter and the consequent changes in the electronic states. From reflection, transmission and absorption processes it is possible to evaluate the optical constants refractive index (n), extinction coefficient (k) and absorption coefficient (Ŭ) and in turn also the complex dielectric constant (‘*) of a solid state thin films [8].

4.6.1 Absorption co-efficient

When a semiconductor is illuminated by light, photon strikes the surface, a function of photons is reflected and the remaining photon enters the semiconductor. Some of these are absorbed within the semiconductor and the remainder transmitted into the semiconductor. The absorption of radiation by any medium occurs through the excitation of electrons and photons. For semiconductor, it is convenient to consider several types of absorption arising form

i) Electronic transitions between different energy bands.

ii) Electronic transitions within any energy band.

iii) Electronic transition to localized states of impurity atoms.

iv) Lattice vibrations.

v) Vibrations of impurity atoms

In the fundamental absorption region the transmission T is given by

$$T = A\exp\left(-\frac{4\pi kt}{\lambda}\right) \qquad 4.3$$

Where A is constant, k is the extinction co-efficient and t is the thickness. For $k^2 << n^2$, the principal variation of T occurs in the exponential term and pre-exponential term A. Therefore

$$T \approx \exp(-\alpha t) \qquad 4.4$$

Where $\alpha = -\frac{4\pi k}{\lambda}$ is the absorption coefficient of the film. Thus the value of absorption coefficient may be calculated from the relation [9].

$$\alpha = \frac{\ln \frac{1}{T}}{t} \qquad 4.5$$

4.6.2 Direct band gap of semiconductor

If the maximum of the valance band and the minimum of conduction band energy exist for the same value of crystal momentum P in a semiconductor, then the semiconductor is called direct band gap semiconductor.

The form of the absorption process for a direct band gap semiconductor is shown in energy momentum sketch of Fig.(4.5). Since the momentum of photon small compared to the crystal momentum, the latter essentially is conserved in the transition. The energy difference between the initial and the final state equal to the energy of the original photon

i.e. E_f ï $E_i = h\nu$ 4.6

interms of parabolic band.

$$E_f \text{ ï } E_c = \frac{P^2}{2m_c^*} \qquad 4.7$$

Therefore the specific value of crystal momentum at which the transition occur is given by

$$\left(E_f - E_i\right) - \left(E_C - E_V\right) = \frac{P^2}{2}\left[\frac{1}{m^*_c} + \frac{1}{m^*_n}\right] \qquad 4.8$$

$$h\nu - E_g = \left[\frac{1}{m^*_c} + \frac{1}{m^*_n}\right] \qquad 4.9$$

Where, $h\nu = E_f$ ï E_i = photon energy and $E_g = E_c - E_v$ = Energy gap.

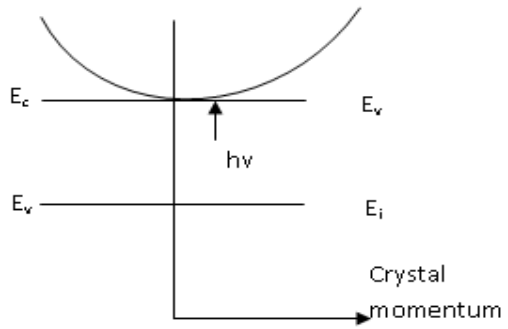

Fig. 4.5: Energy-crystal momentum of an direct band gap semiconductor.

As the photon energy, hν increases, so does the value of the crystal momentum at which the transition occurs Fig:(4.5). The energy form the band edge of both the initial and the final states also increases. The probability of absorption depends on the density of the electron at the energy corresponding to the initial state as well as the density of empty states at the final energy. Since both these quantities increase with energy away from the band edges the absorption co-efficient increase rapidly with increasing photon energy above E_g. A simple theoretical treatment gives the result, as

$$\alpha (h\nu) \approx A^* (h\nu - E_g)^{\frac{1}{2}} \qquad 4.10$$

Where A^* is a constant having the numerical value of 2×10^4 when α is expressed in cm^{-1}, hν and E_g in electron volts (eV) [10].

4.6.3 Refractive index and extinction coefficient

The refractive index of a substance is a measure of the speed of light in that substance. Refractive index defined is the ratio of the velocity of light through a vacuum to the velocity of light through the medium.

A simple mathematical description of the refractive index is as follows:

n = speed of light in a vacuum / speed of light in medium

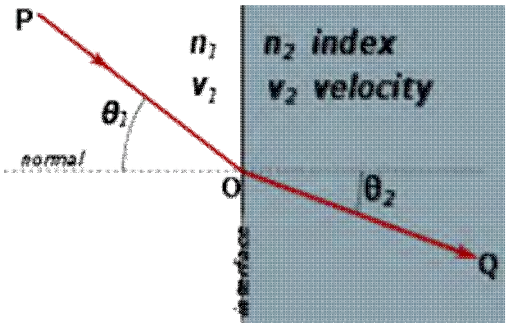

Fig. 4.6: Refraction of light at the interface between two media

Let us consider a thin film of thickness t having a refractive index n. If the absorption occurs then n should be replaced by n_o-*ik* i.e., $n = n_o$-*ik*

where, k is the extinction coefficient and n_o is the real part of n. The physical meaning of k is the following. When the wave has propagated over a distance equal to the wavelength in the vacuum, the amplitude is reduced by a factor exp(-2´ k).

There are many methods for determination of n and measuring transmittance and reflectance of the same film can make k separate determination of n and k. We can determine absorption coefficient by using the relation,

$$\alpha = \left(\frac{4\pi k}{\lambda}\right) = \frac{1}{t}\ln\left[\frac{(1-R)^2}{T}\right] \qquad 4.11$$

From above equation we can write,

$$k = \frac{\alpha\lambda}{4\pi} = \frac{\lambda}{4\pi t}\ln\left[\frac{(1-R)^2}{T}\right] \qquad 4.12$$

Where ɔ is the wavelength of incident light and T is the transmittance.

The refractive indices, n for the films having interference in the reflectance spectra can be determined by the relation,

$$n = \frac{1}{2t}\left[\frac{\lambda_1\lambda_2}{\lambda_2 - \lambda_1}\right] \qquad 4.13$$

Where t is the thickness of the film and λ_1 and λ_2 are the wavelengths of two consecutive maxima of interference pattern. The same value of n can be determined by the relation,

$$n^2 = n_0 n_s \left[\frac{1 \pm \sqrt{R_{qw}}}{1 \pm \sqrt{R_{qw}}} \right] \qquad 4.14$$

Where n_o and n_s are refractive index of air and glass substrate respectively and R_{qw} is the reflectance of the quarter wavelength .

The refractive index n and the extinction coefficient k in the crystal are related to the reflectivity at normal incidence by the relation,

$$r = \frac{n + ik - 1}{n + ik + 1} \qquad 4.15$$

and the reflectance is given by the relation,

$$R = rr^* = \frac{(n-1)^2 + k^2}{(n+1)^2 + k^2} \qquad 4.16$$

From equation we can write,

$$n = \frac{-2(R+1) \pm \sqrt{(2R+2)^2 - 4(R-1)(R + Rk^2 - k^2 - 1)}}{2(R-1)} \qquad 4.17$$

Knowing reflectance R and extinction coefficient k, we can calculate refractive index by using equation [11].

4.7 Electrical Properties

4.7.1 Resistivity and conductivity measurement

Surface resistivity could be defined as the materialôs inherent surface resistance to current flow multiplied by that ratio of specimen surface dimensions (width of electrodes divided by the distance between electrodes) which transforms the measured resistance to that obtained if the electrodes had formed the opposite sides of a square. In other words, it is a measure of the materialôs surface inherent resistance to current flow. Surface resistivity does not depend on the physical dimensions of the material.

According to Ohmôs law for circuit theory, the resistance of a material is the applied voltage divided by the current drawn across the material across two electrodes.

$$R = V/I \qquad 4.18$$

Where:

R=Resistance (ohms, Ý)

V= Voltage (volts, V)

I = Current (amperes, A)

The resistance per unit length of unit cross section is called resistivity. It is denoted by ρ and mathematically defined as,

$$\rho = \frac{RA}{L} \qquad 4.19$$

Where A is the cross-sectional area and L is the length [11].

Electrical conductivity of a material is reciprocal of resistivity of the material. It is denoted by σ and mathematically defined as

$$\sigma = \frac{1}{\rho} \qquad 4.20$$

Resistivity is an intrinsic property of a material and depends only on the crystal structure of the material. The resistivity can be obtained by measuring the resistance of a specimen of the material with well-defined regular geometric shape [12]. There are many methods to measure resistivity. Some of them have been discussed below.

4.7.2 Methods to determine the resistivity

There are some methods commonly used for the measurement of resistivity.

A) Two-probe method

B) Four probe method

C) Van-der Pauw method

4.7.2.1 Two-probe method

In this method potential is applied between the two ends of the specimen and the voltage drop is measured between two points in the specimen. The method is generally used to determine the high resistivity i.e., low conductivity having order 10^{-14} to 10^{-18} mho-cm^{-1}. The voltage drop is measured between potential probe as shown is Fig (4.7).

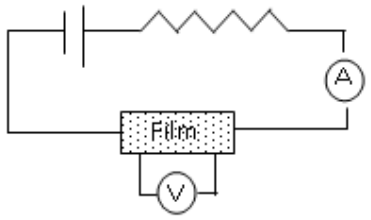

Fig. 4.7: Two probe method

4.7.2.2 Four-probe technique

Four-probe method is usually used for the determination of low resistivities. For this purpose four metal pins at a equal distance D are pressed by springs against the semiconductor sample as shown in Fig. (4.8). If the outside pins carry a current of intensity, I a voltage drop is measured between the inner probes of magnitude V.

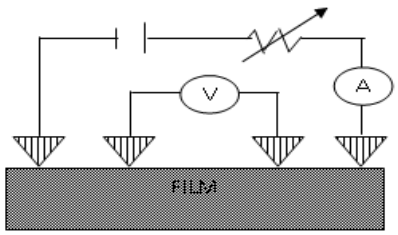

Fig. .4.8: Four-probe method

Assuming the sample to be much thicker that the pin distance, D the resistivity ρ is given by

$$\rho = \frac{2\pi DV}{I} \qquad 4.21$$

The effect of the contact resistance is avoided in Four-probe method.

4.7.2.3 Van-der Pauw method

The resistivity of a film having any arbitrary shape can be uniquely determined by Van-der Pauwôs method. A brief account of this method is given below because in our measurement we have used Van-der Pauw method.

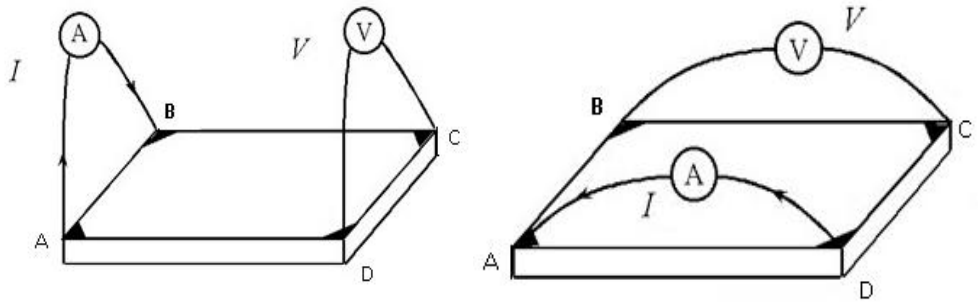

Fig. 4.9: Van-der Pauw method

At first we select a region or the sample where four electrical contacts were made at Four Corners, say A, B, C, and D as shown in Fig. (4.9). Using silver paste or indium was used to make the contact. If a current I_{AB} entering the specimen through the contact A and leaving through the contact, B produces a potential difference $V_D - V_c$ between C and D then the resistance $R_{AB, CD}$ is defined as

$$R_{AB.CD} = \frac{V_D - V_C}{I_{AB}} = \frac{V_{CD}}{I_{AB}}$$

Similarly, $R_{BC.DA} = \quad = \frac{V_A - V_D}{I_{BC}} = \frac{V_{DA}}{I_{BC}}$

$$R_{CD.AB} = \frac{V_B - V_A}{I_{CD}} = \frac{V_{AB}}{I_{CD}}$$

and $$R_{DA.BC} = \frac{V_C - V_B}{I_{DA}} = \frac{V_{BC}}{I_{DA}}$$

The resistivity of a thin film can be expressed by the equation

$$\rho = \frac{\pi t}{\ln 2}\left[\frac{R_{AB.CD} + R_{BC.AD}}{2}\right] \times f\left[\frac{R_{AB.CD}}{R_{BC.AD}}\right] \qquad 4.22$$

$$\rho = 4.53t \times \left[\frac{R_{AB.CD} + R_{BC.AD}}{2}\right] \times f\left[\frac{R_{AB.CD}}{R_{BC.AD}}\right] \qquad 4.23$$

where t is the thickness of the film and the function f can be evaluated from the equation

$$\left[\frac{R_{AB.CD} - R_{BC.DA}}{R_{AB.CD} + R_{BC.DA}}\right] = \frac{f}{\ln 2} are\cosh \frac{\exp(\ln 2 / f)}{2} \qquad 4.24$$

If $R_{AB,CD}$ and $R_{BC,DA}$ are almost equal, f may be approximately equal to unity and then the equation (4.19) takes the form,

$$\rho = 2.265\ t\ (R_{AB,CD}+R_{BC,DA})\ \text{Ohm-cm} \qquad 4.25$$

It is very difficult to get f, equal to unity, so we have taken the value of ófô from the chart for different ratio greater than unity.

4.7.2.4 Activation energy

The energy required to transfer charge from one neutral island to another is known as 'activation energyô and is denoted by ΔE . This is equivalent to the electrostatic binding energy of the charge to the island. When these charge carries are excited to at least this energy from the Fermi level, there will be tunneling from one island to another. These island or small particles are called crystallites.

The activation energy is related with film conductivity [13] and given by the relation

$$\sigma = \sigma_o \exp\left(\frac{-\Delta E}{kT}\right) \qquad 4.26$$

Where ΔE is the activation energy, K is the Boltzmann constant and T is the absolute temperature. Eq. (4.26) can be written as,

$$\ln \sigma = \left(\frac{-\Delta E}{kT}\right) + \ln \sigma_o \qquad 4.27$$

The activation energy ΔE is calculated from the slope of a curve ln σ vs. (1/T). Therefore the activation energy ΔE is given by

$$\Delta E = -\frac{\ln \sigma}{1/T} k \qquad 4.28$$

4.8 Methods of Film Thickness Measurement

4.8.1 Introduction

In thin film experiments, thickness measurement is an essential job. All most all the electrical parameters except the Hall mobility and sheet resistance and also optical parameters need for their evaluation the value of film thickness should be measured with precision as far as possible. Some of the common methods of measurement of film thickness here we used Fizeu Firngs method.

4.8.2 Fizeau fringes Method

Weiner was the first to use interference fringes to measure film thickness. When two reflecting surfaces are brought into close proximity, interference fringes are produced, the measurement of which makes possible a direct determination of film thickness and surface topography with high accuracy. In this method, two types of fringes are utilized for thickness measurement. The first produces Fizeu fringes of equal thickness, using a monochromatic light source. The second uses a white light source and produces fringes of equal chromatic order. To make the Fizeau fringes of equal thickness visible in a multiple beam interferometer formed by a thin absorbing film on a glass substrate. But if the experimental sample is transparent with a very smooth surface no such auxiliary coating is necessary.

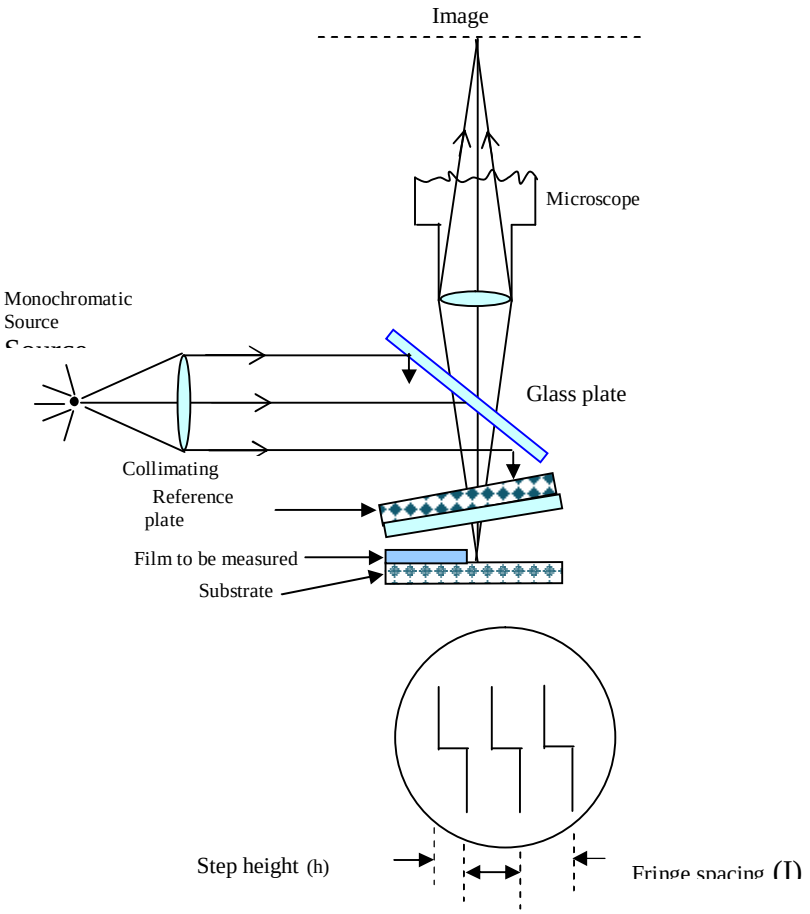

Fig. 4.10 : Interferometer arrangement for producing reflection Fizeau fringes of equal thickness.

This illuminated with a parallel monochromatic beam of light a fringe system as shown in Fig. 4.9 is produced. The displacement ôhô of the fringe system across the film substrate step is then measured to calculate the film thickness ôtô using the relation

$$t = \frac{h}{frings - pacing} \times \frac{\lambda}{2} \qquad 4.29$$

Where λ be the wavelength of the monochromatic light employed. If the fringe spacing is ôlô then we can written as

$$t = \frac{h\lambda}{2l} \qquad 4.30$$

References

1. Huang X., Guanghai Li, Cao B., Wang M., and Hao C., ñMorphology Evolution and CL Property of Ni-Doped Zinc Oxide Nanostructures with Room-Temperature Ferromagnetismò J. Phys. Chem. C., Vol. 113, P. 4381ï 4385, 2009.

2. Ximello-Quiebras J. N., Mejía-García C., Caballero-Rosas A., Hernández-Contreras H., Contreras-Puente G., Vidal and Pascher H., ñPhotomodulation study in CdS thin films grown by sputtering in a large areaò J. Appl. Phys. Lett. Vol. 431-432, P. 223-225, 2003.

3. Moutinho H. R, Albin D, Yan Y, Dhere, Perkins C., and Al-Jassim M. M., ñA Comparative Study of CdS Thin Films Grown by Chemical-Bath Deposition and Close-Spaced Sublimationò Renewable Energy Lab., United States R.G. vol .54. 2005.

4. Lupan O., Shishiyanu S., Chow, Shishiyanu T.,ñNanostructured zinc oxide gas sensors by successive ionic layer adsorption and reaction method and rapid photothermal processingò Thin Solid Films, Vol. 516, P. 3338ï 3345, 2008.

5. Kang S. J., Joung Y. H., Shin H. H., Yoon Y. S., ñEffect of substrate temperature on structural, optical and electrical properties of ZnO thin films deposited by pulsed laser depositionò J Mater Sci.: Mater. Electron, Vol. 1, P. 1073ï 1078, 2008.

6. Raviprakash Y., Kasturi, Bangera V., Shivakumar G. K., ñPreparation and characterization of CdxZn1_xS thin films by spray pyrolysis technique for photovoltaic applicationsò Solar Energy, Vol. 83, p. 1645ï 1651, 2009.

7. Islam M. R., and Podder J., ñOptical Properties of ZnO nano fiber thin films grows by spray pyrolysis of zince acetate precursorò Cryst. Res. Technol., Vol. 44, No.3, P. 286-292, 2009.

8. Khan M. K. R., Rahman M. A., Shahjahan M., Rahman M. M., Hakim M. A., Saha D. K., and Khan J. U., ñEffect of Al-doping on optical and electrical properties of spray pyrolytic nano-crystalline CdO thin filmsò Current Appl. Phys., Vol.10, P. 790ï 796, 2010.

9. Shimono D., Tanaka S., Torikai T., Watari T., and Murano M., ñPreparation of transparent and conductive ZnO films using a chemical solution deposition processò J. of Ceramic Prog. Res., Vol. 2, No. 4, P. 184-188, 2001.

10. Buba A. D. A., and Adelabu J. S. A., ñOptical and Electrical Properties of Chemically Deposited ZnO Thin Filmsò. The Pacific J. of Sci. and Technol., Vol. 11, Num. 2 , 2010.

11. Tsai P. P., Bresee R. R., ñ Using field theory to Measure Surface Resistivity of High ï Resistance Polymeric Films,ò J. of Appl. Polymer Sci., Vol. 82, No.11, P. 2856-2862, 2001.

12. Choudhury, M. G. M., Islam, M. R., Rahman, M. M., Hakima, M. O., Khana, M. K. R., Kaob, K. J.,and Laib, G. R., ñ Preparation Adn Characterization Of ZnSe:Al Thin Filmsò Acta Phys. Slov., Vol. 54, No. 4, P. 417-425, 2004.

CHAPTER- V

EXPERIMENTAL RESULTS AND DISCUSSION

CHAPTER- V

EXPERIMENTAL RESULT AND DISCUSSIONS

5.1 Introduction

The results obtained from different experimental measurements of the Ni doped ZnO polycrystalline thin films have been provided in this chapter. The possible explanations and discussions of the results of Ni-doped ZnO thin films have been given in this section.

5.2 Surface morphology

Scanning electron microscopy is a convenient technique widely used to obtain the surface morphological information of thin films. Surface morphology of pure ZnO and Ni doped ZnO films on glass substrate were studied by scanning electron microscopy (SEM). Figure (5.1 and 5.2) shows the surface morphology of as-deposited ZnO and Ni doped ZnO thin films 5000X to 10000X magnifications respectively. The films were found uniform and well covered on the glass substrate surface.

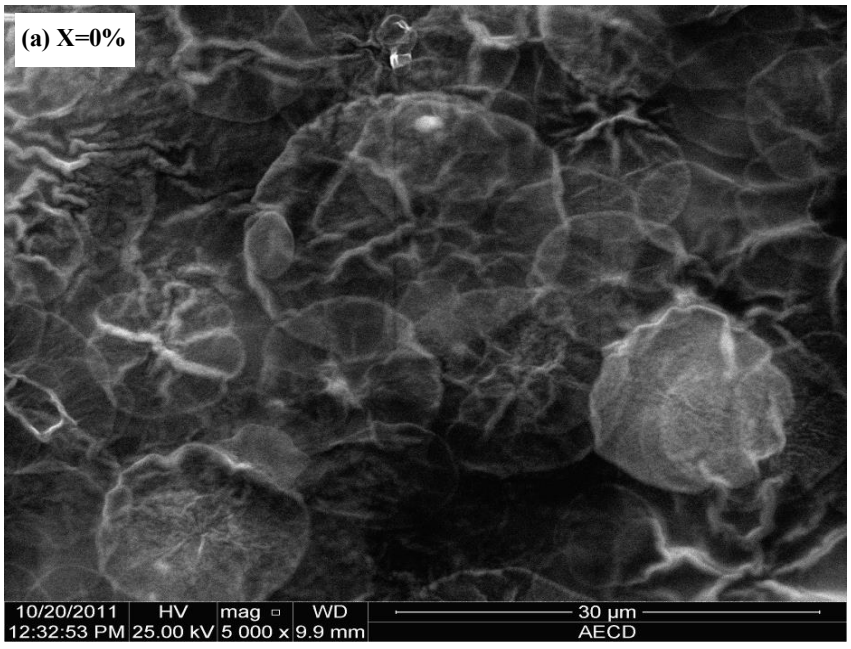

Fig. 5.1a: SEM image of (5000X magnification) $Zn_{1-x}Ni_xO$ thin films for (a) x = 0%

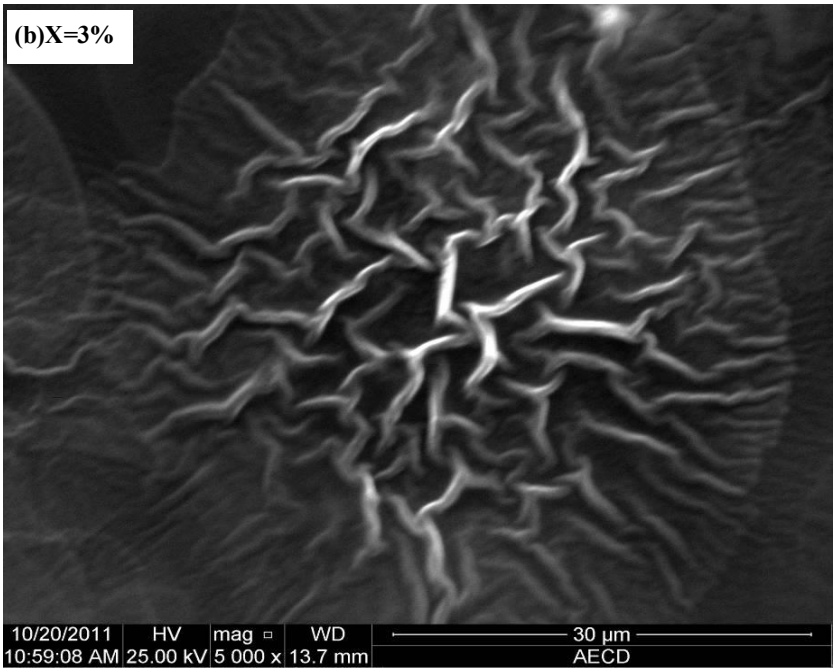

Fig. 5.1b: SEM image of (5000X magnification) $Zn_{1-x}Ni_xO$ thin films for (b) x= 3%

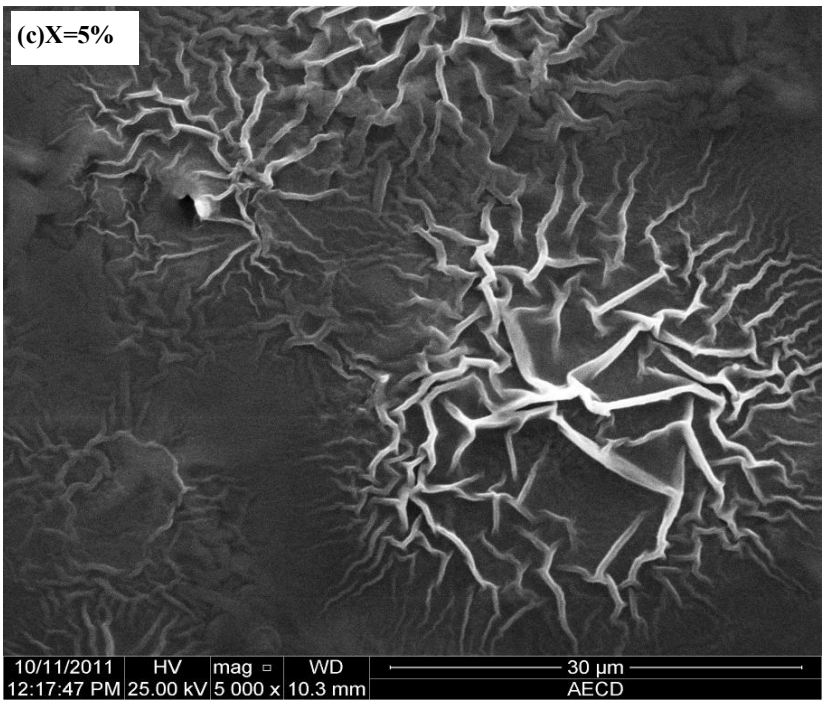

Fig. 5.1c: SEM image of (5000X magnification) $Zn_{1-x}Ni_xO$ thin films for (c) x=5%

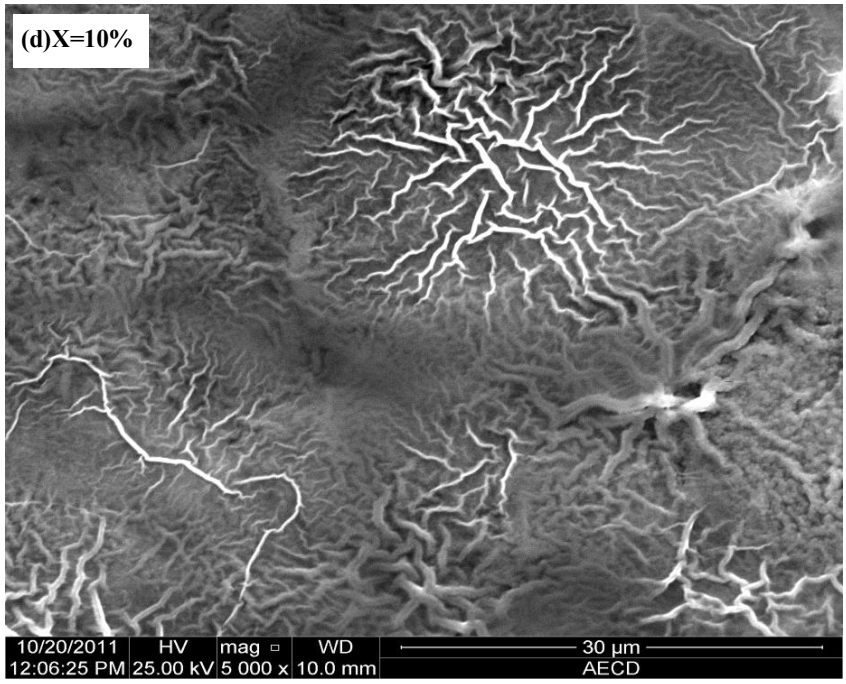

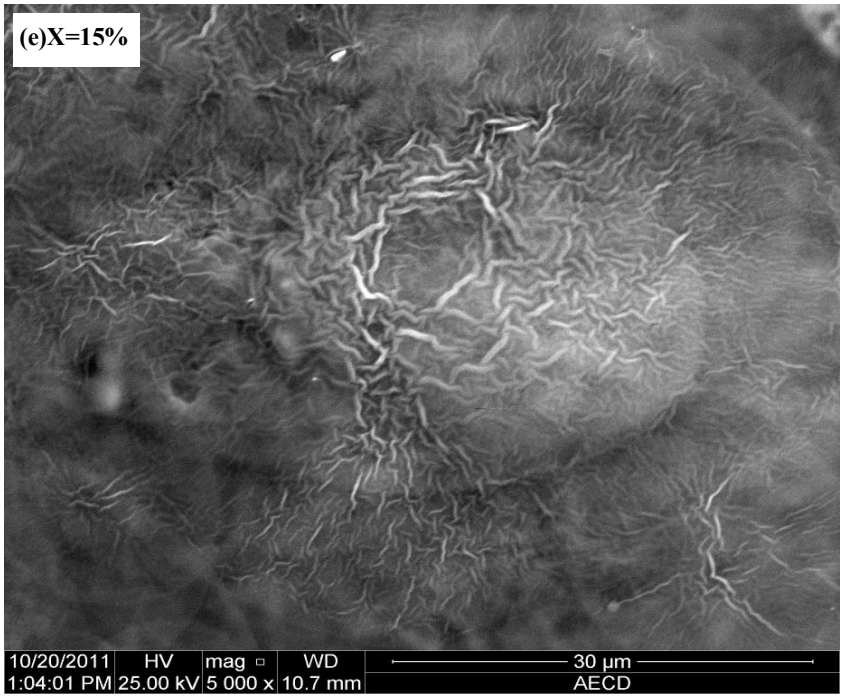

Fig. 5.1 d and e: SEM images of (5000X magnification) $Zn_{1-x}Ni_xO$ thin films for (d) x=10% and (e) x=15%

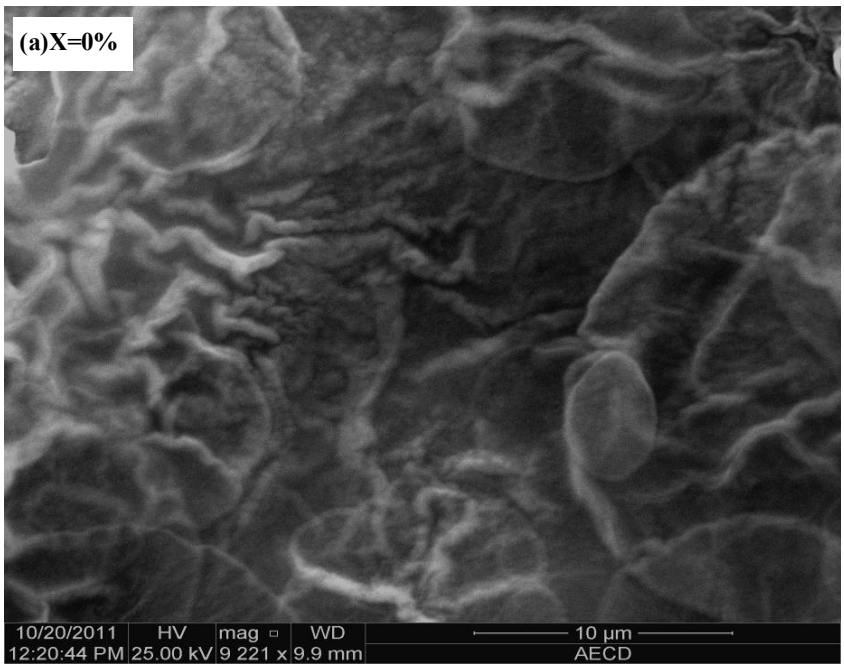

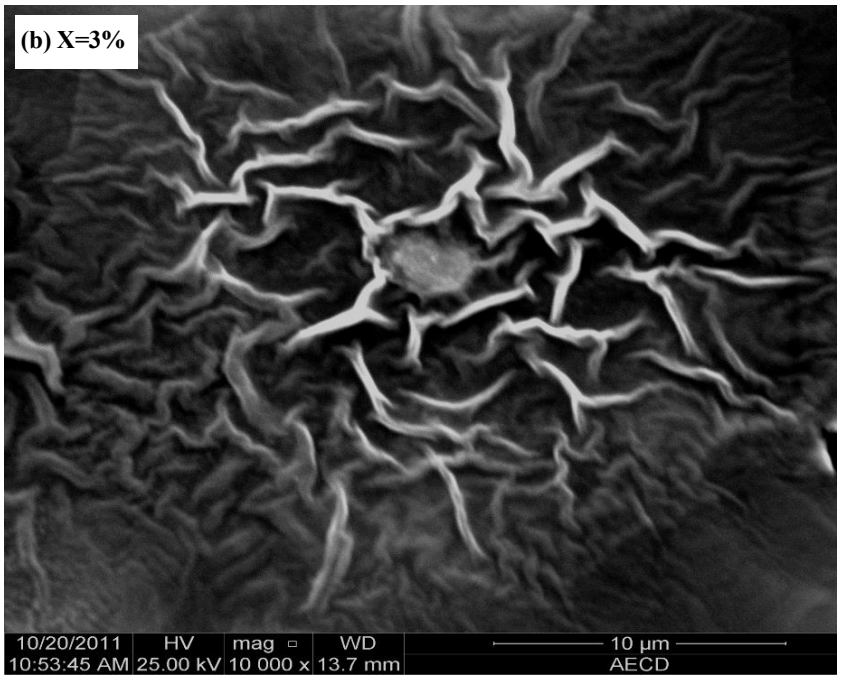

Fig. 5.2 a and b: SEM images of (10,000X magnification) $Zn_{1-x}Ni_xO$ thin films for (a) x=0% and (b) x=3%

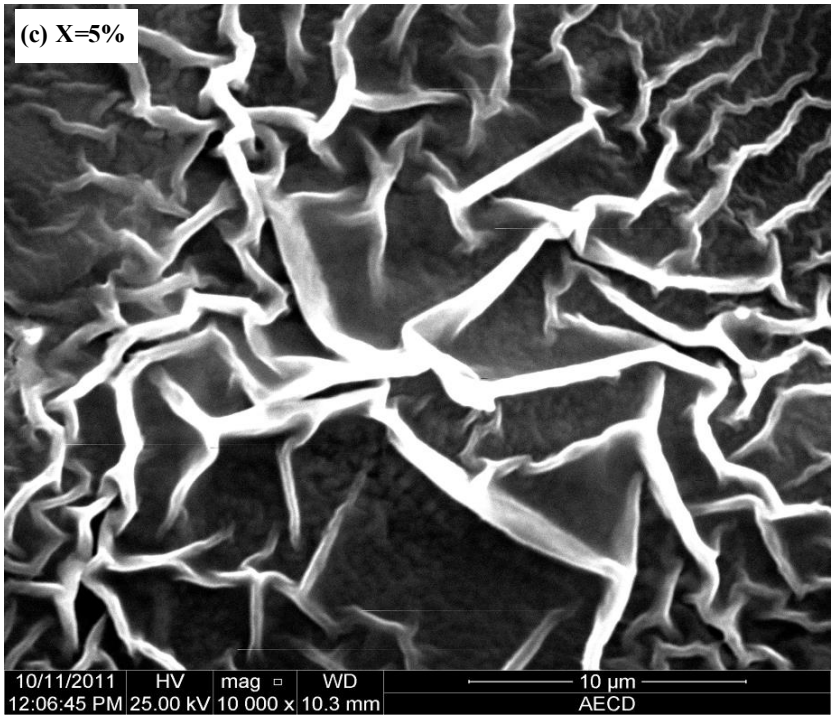

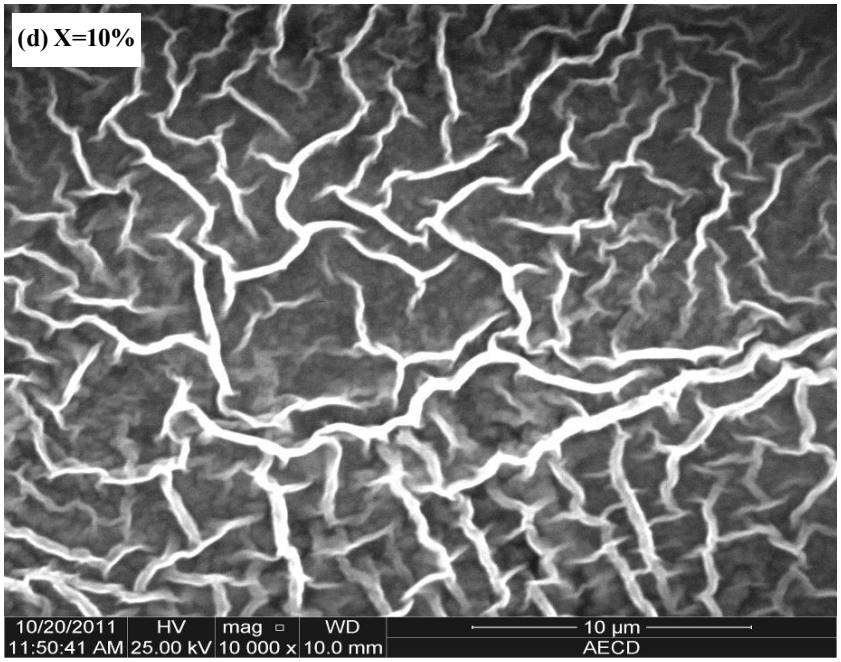

Figs. 5.2 c and d: SEM images of (10,000X magnification) $Zn_{1-x}Ni_xO$ thin films for (c) x=5% and (d) x=10%

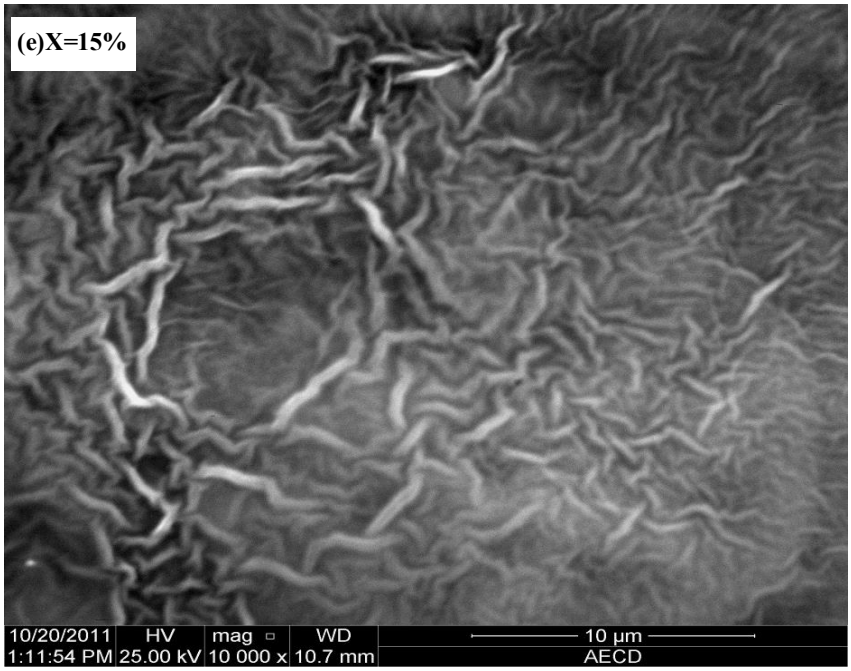

Figs. 5.2e: SEM image of (10,000X magnification) $Zn_{1-x}Ni_xO$ thin films for (e) x=15%

Under higher magnifications, the SEM micrograph of the ZnO and Ni doped ZnO films shows figs. (5.1 and 5.2) high density of closely packed smooth ganglia like fibers over a large area around the nucleation center [1]. The fibers are randomly oriented of various lengths around the nucleation center. Typical length of the fiber varies from 2.0 ε m to 2.5 ε m.

5.2 Compositional studies

The quantitative analysis of the as-deposited ZnO and Ni doped ZnO thin films carried out by EDX are shown in Figure 5.3a. Two strong peaks corresponding to Zn and O were found in the spectrum, which confirms the high purity of the ZnO thin film. At high operating voltage the electron beam penetrates the film and reaches the glass surface, which results the Si peak. Figures (5.3a, 5.3b, 5.3c and 5.3d) are shown the EDX analysis spectrum for $Zn_{1-x}Ni_xO$ (x=3%, 5%, 10%, and 15%) thin films.

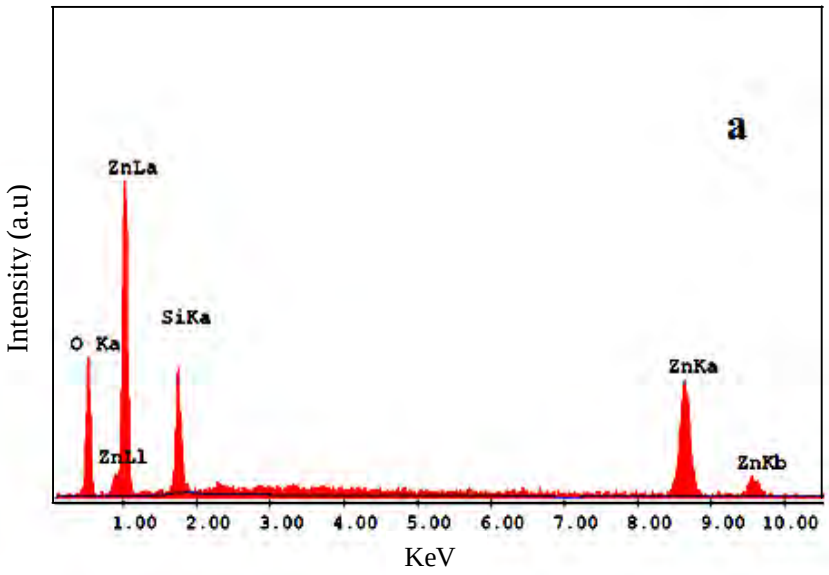

Fig. 5.3a: Elemental analysis of as-deposited ZnO film on to glass

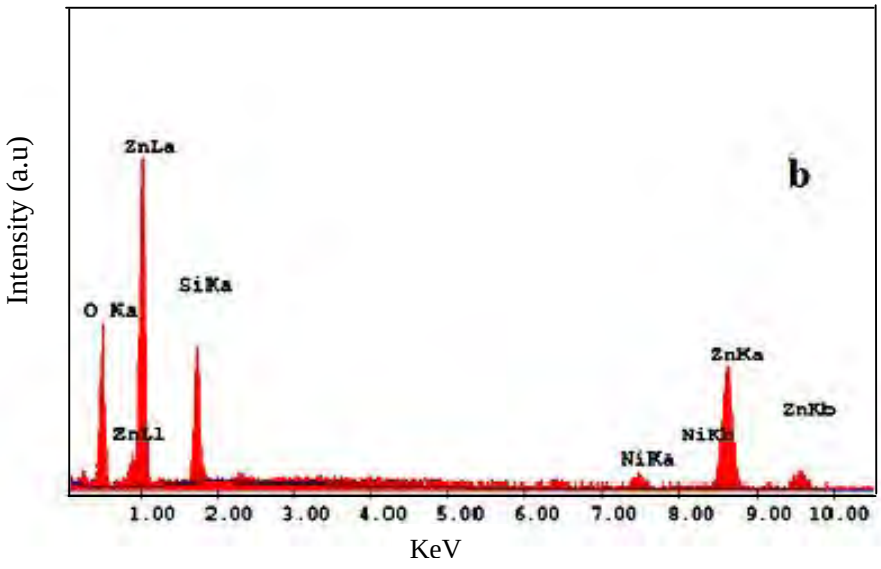

Fig 5.3b : EDX spectrum of $Zn_{1-x}Ni_xO$ thin film for x=3%

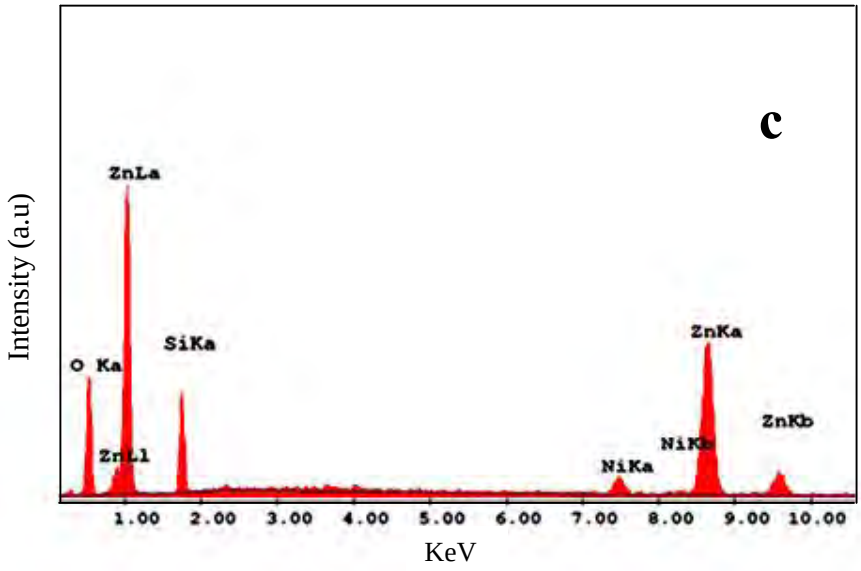

Fig. 5.3c: EDX spectrum of $Zn_{1-x}Ni_xO$ thin films for x=5%

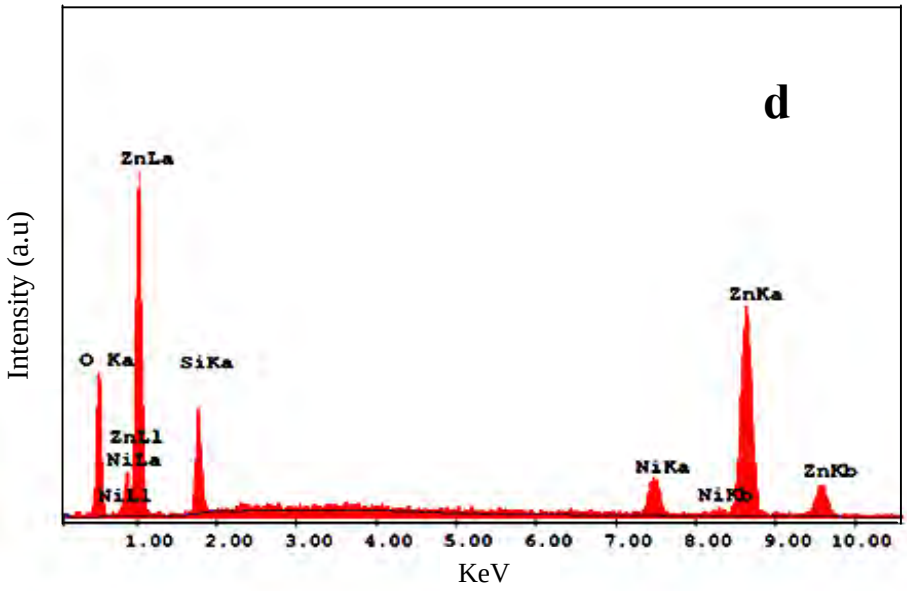

Fig. 5.3d: EDX spectrum of $Zn_{1-x}Ni_xO$ thin film for x=10%

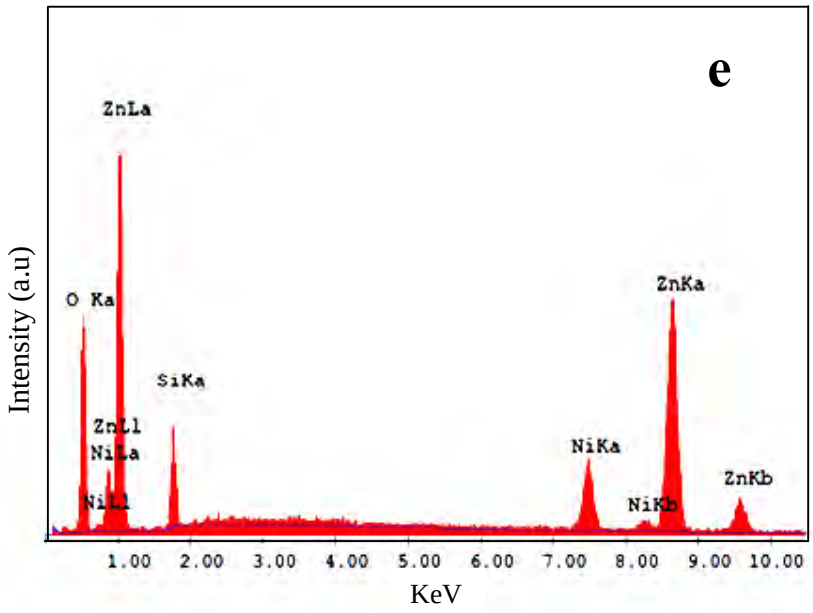

Fig .5.3e: EDX spectrum of $Zn_{1-x}Ni_xO$ thin film for x=15%

Table 1: EDX analysis data for $Zn_{1-X}Ni_XO$ thin films.

Concentration Ni (%)	Elements	Wt%	At%
0	Zn	87.44	67.66
	O	7.08	22.51
	Si	5.49	9.83
3	Zn	85.01	63.22
	Ni	2.69	2.92
	O	6.66	23.58
	Si	5.84	10.25
5	Zn	84.08	79.25
	Ni	3.96	3.74
	O	6.40	15.63
	Si	5.57	1.36

Concentration Ni (%)	Elements	Wt%	At%
10	Zn	83.29	78.95
	Ni	7.56	6.45
	O	3.89	14.05
	Si	5.26	0.54
15	Zn	79.47	72.37
	Ni	10.30	9.83
	O	4.90	17.15
	Si	5.31	0.63

The compositional analysis data shows the good controllability of $Zn_{1-x}Ni_xO$ composition thin films by locally made low cost Spray Pyrolysis deposition technique.

5.4 XRD Analysis of Thin Films

The structural properties of undoped ZnO and Ni-doped ZnO films on glass substrates are investigated by X-ray diffraction patterns. The XRD patterns of the films were taken using λ = 1.79 Å (CO K_{α}) source. XRD patterns of as deposited ZnO and Ni doped ZnO films at various concentrations are shown in figs.(5.4). All peaks in this figure could be identified as a ZnO phase with a hexagonal wurtzite crystal structure. From the figures it is observed that the films are polycrystalline nature in all cases. The characteristic peaks were identified at 2θ = 37.45°, 40.55°, 42.60°, 52.70°, 55.85° and 63.10° having (*hkl*) value (100), (002), (101), (102), (110) and (103) respectively [2].

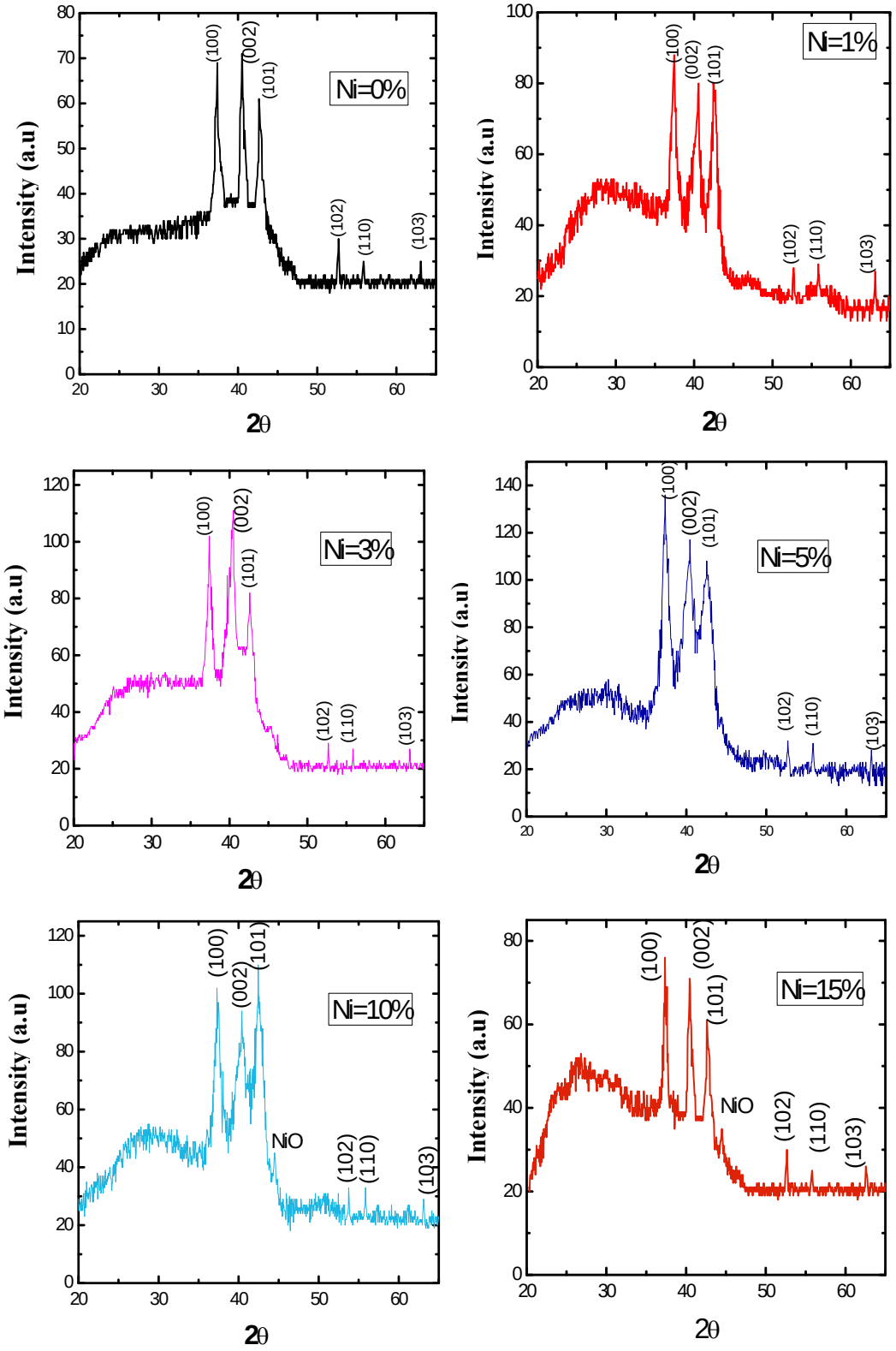

Fig. 5.4: XRD patterns for ZnO and Ni doped ZnO thin films for different Ni concentrations

The peak intensity increases from 0% to 5% and then decreases with the increase of Nickel concentration. A secondary phase of NiO has been observed in above 5% of Ni doped sample [3]. Crystallite size of the structure was calculated using the relation [4].

$$D = 0.94\lambda/B\cos\theta \quad (5.1)$$

Where, D is the crystallite size, λ is the wavelength of the X-ray used, θ is the diffraction angle and β is the full width at half maximum (FWHM). Crystallite sizes of the deposited films have been calculated using (100) plane. The values of crystallite sizes are obtained 20 nm for pure ZnO and 10 nm, 16 nm, 11 nm, 13 nm and 11 nm for ZnO:Ni samples with Ni concentrations 1%, 3%, 5%, 10% and 15%, respectively [5]. The grain size values with different Ni concentrations are given in the following Table-2. The decrease in crystalline quality is attributed to the effect that all Ni does not go to the Zn lattice sites, which reduces the crystallinity of the ZnO:Ni structure. The values of grain size with different Ni concentrations are given in the following Table -2.

Table 2: Crystallite size of $Zn_{1-x}Ni_xO$ films deposited on glass substrates.

x in %	**a (Å)**	**c (Å)**	**c/a ratio**	**Grain size (nm)**
0%	3.2195	5.1661	1.6046	20
1%	3.2237	5.1722	1.6044	18
3%	3.2278	5.1722	1.6023	16
5%	3.2278	5.1784	1.6043	11
10%	3.2319	5.1844	1.6041	13
15%	3.2278	5.1784	1.6043	14

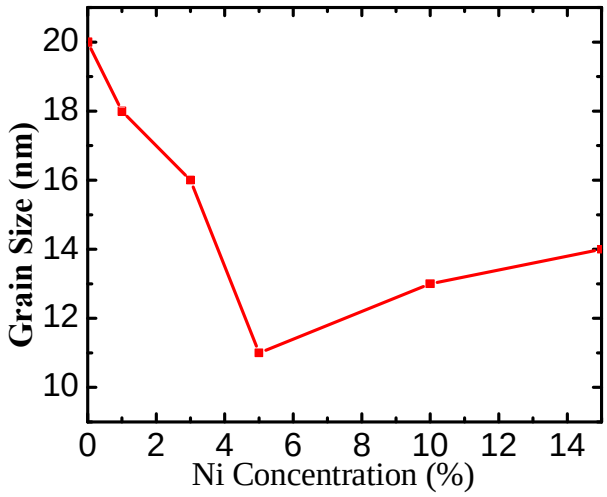

Fig. 5.5: Grain size Vs Concentration Ni in Ni doped ZnO thin films.

Lattice constant slightly vary with doping concentration of Ni but no linear relation with Ni concentration. From the table-2 it is widely varied for different samples. It may dependent on doping concentration or on the parameters of film preparation.

5.5 Optical Properties

5.5.1 Transmission

The optical transmission spectra are shown in fig. 5.5 with wavelength range 250 nm -1100 nm. The figure shows the variation of transmittance with the doping concentration of Ni. In the visible region, the $Zn_{1-x}Ni_xO$ films show good transparency and have an average transmittance above 55% to 80% depending on the Ni concentration. These spectra show high transmittance in the wavelength range from 500 nm -1100 nm. Below 500 nm there is a sharp fall of transmittance of the films.

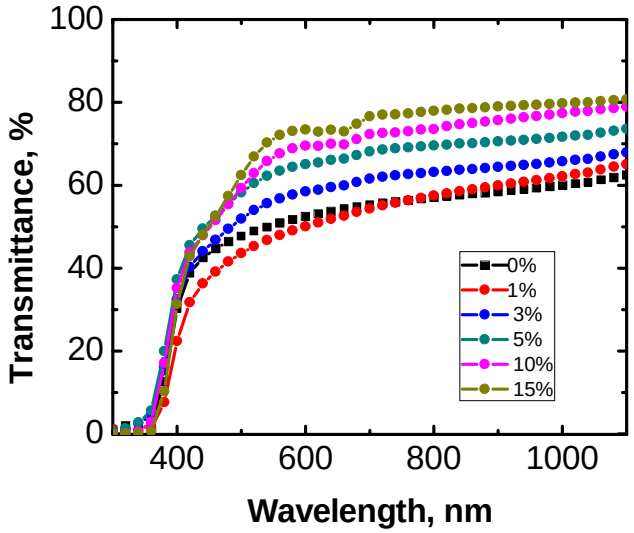

Fig. 5.6: Transmittance vs. wavelength of $Zn_{1-x}Ni_xO$ thin films.

5.5.2 Absorbance

The optical absorption spectra are shown in fig. 5.7 with wavelength range 250 nm -1100 nm. The figures show the variation of absorbance with the doping concentration of Nickel. From the figure it is seen that the optical absorption decreases with the doping concentration of Nickel of the $Zn_{1-x}Ni_xO$ thin films [6].

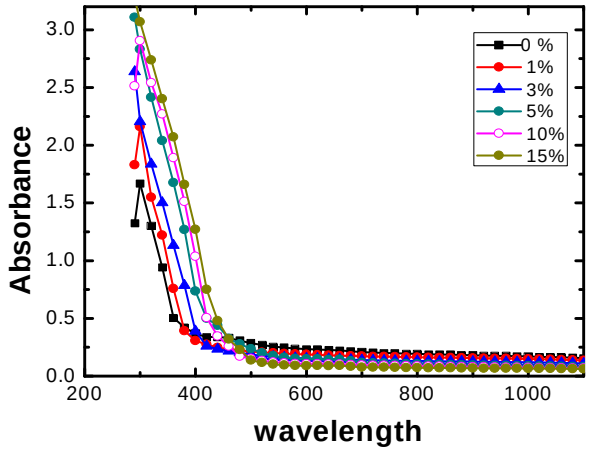

Fig.5.7: Variation of optical absorbance with wavelength of $Zn_{1-x}Ni_xO$ thin films.

5.5.3 Optical band gap

The optical band gap can be determined by analyzing the transmission data using the classical relation [7],

$$\alpha h\nu = A\,(h\nu - E_g)^n \qquad 5.2$$

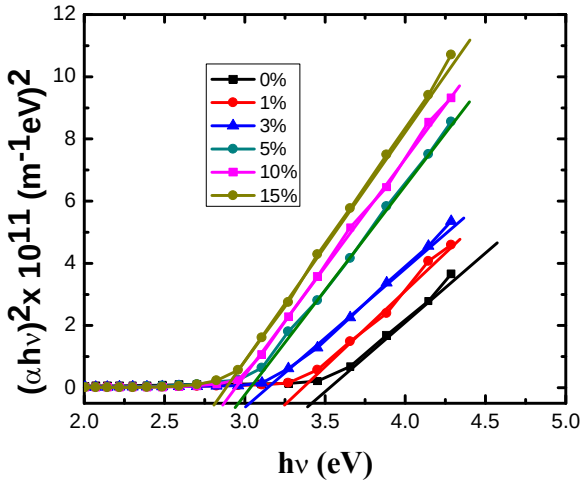

Fig.: 5.8: Variation of $(\check{U}h\nu)^2$ with photon energy for different doping concentration of Ni in ZnO thin films.

where, A is a constant, ñhνò is the photon energy and ñE_gò is the optical band gap of the semiconductor and ñnò is index related to the density of states for the energy

band and is determined by the nature of optical transition involved in the absorption process. For the determination of band gap we have considered the direct (n = 2) transitions. Variation of $(\alpha h\nu)^2$ with $h\nu$ for different doping concentration of Ni doped ZnO thin films are shown in fig. (5.8). The band gap of the sample were obtained from intercept on energy axis after extrapolation of the straight-line section in the high-energy region of $(\alpha h\nu)^2$ vs. $h\nu$ curve [8]. For direct transition the observed optical band gap depends on the doping concentration and varies from 3.38 eV to 2.80 eV.

Table 3: Variation of band gap of $Zn_{1-x}Ni_xO$ thin films with different doping concentration of Ni.

Sample	Concentration of Ni (%)	Direct band gap E_g in eV
$Zn_{1-X}Ni_XO$	0	3.38
	1	3.30
	3	3.05
	5	2.95
	10	2.90
	15	2.80

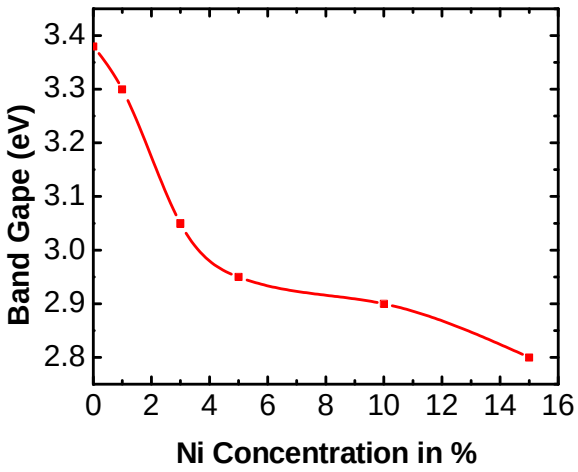

Fig. 5.9: Variation of direct band gap energies with doping concentration of $Zn_{1-x}Ni_xO$ thin films

Small amount of Nickel present in the films greatly affects the optical band gap. The energy gap decreases as the Ni concentration increases [9]. From fig.(5.9) the band gap of 5% Ni doped sample demonstrates that some lower concentration of Ni is incorporating into the ZnO matrix. The results due to sp-d exchange interactions between band electron and localized d electrons of the Nickel ions substituting for Zinc ions.

5.5.4 Refractive index and extinction coefficient

The refractive index and extinction coefficient are determined by computing the transmission and reflection data. The variation of refractive index and extinction coefficient with photon energy for $Zn_{1-x}Ni_xO$ thin films are shown in fig. (5.10) and fig.(5.11). From fig.(5.10) it is seen that the refractive index decreases with photon energy and increases with the doping concentration of Ni.

The refractive index has been calculated using the relation [10]

$$n = \left(\frac{1+R}{1-R}\right) + \sqrt{\left(\frac{4R}{(1-R)^2} - k^2\right)} \qquad 5.3$$

Where k is the extinction coefficient and R is the optical reflectance. The refractive index (n) values provide the optical properties of the films. From the figure it is evident that the refractive index increases with the increase of Ni incorporation [11]. From figure it is clear that n decreases rapidly with increasing wavelength from 400 to 500 nm and after that the value of ónôremains constant.

From fig. (5.11) it is seen that the extinction coefficient increases with photon energy and decreases with the concentration of Ni in $Zn_{1-x}Ni_xO$ thin films.

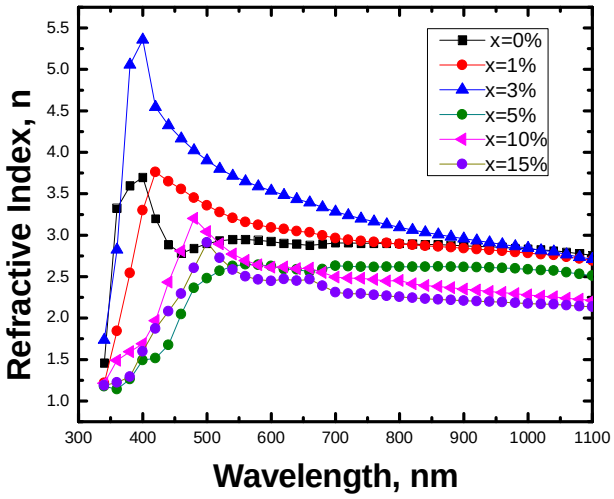

Fig. 5.10: Variation of refractive index with energy for different doping concentration of Ni in ZnO thin films.

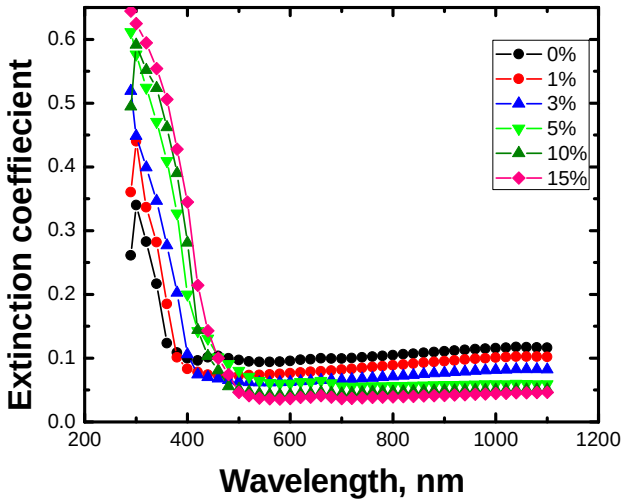

Fig. 5.11: Variation of extinction coefficient with photon energy for different doping concentration of Ni in ZnO thin films.

5.5.5 Optical conductivity

Figure (5.12) shows the variation of optical conductivity with photon energy. Optical conductivity of the thin films have been calculated using the equation

$$\mathring{u} = \breve{U}nc\ /4\acute{}\qquad 5.4$$

Optical conductivity of the $Zn_{1-x}Ni_xO$ thin films decrease with Ni concentration and increases with photon energy.

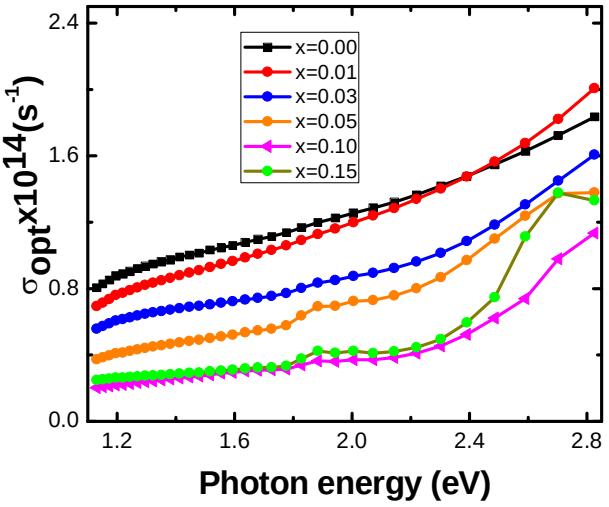

Fig.5.12: Variation of Optical Conductivity with Photon Energy for Zn1-xNixO thin films

5.6 Electrical Properties

5.6.1 Variation of resistivity with temperature

Resistivity of the prepared ZnO and Ni doped ZnO thin films have been measured by Vander Pauws method. The resistivity measurement has been performed over a range from room temperature to 440 K. During the measurement, the temperature increased slowly as a result the whole film is heated with uniform temperature. The variation of resistivity with temperature for films is shown in fig. (5.13).

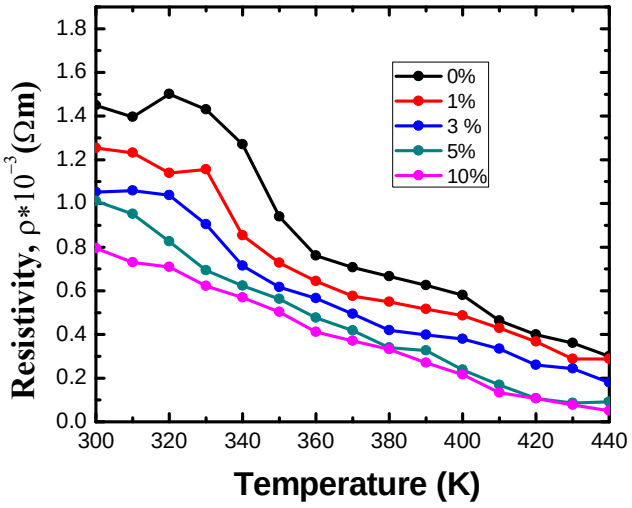

Fig.5.13: Variation of resistivity with respect to temperature for pure and Ni doped ZnO thin films.

The figure shows that the resistivity gradually decreases with the increase of temperature, which indicates the semiconducting nature of the materials. Figure (5.13) also shows that the resistivity decreases with concentration of Ni [12]. This result may be explained as follows: when Ni ($3d^8\ 4s^2$) substitutes the Zn ($3d^{10}\ 4s^2$) site in the ZnO matrix, a free hole is produced and this free hole compensates the electrons of n-type ZnO.

5.6.2 Electrical conductivity

The variations of electrical conductivity with temperature for as deposited doped thin films are shown in fig.(5.14). From the figure it is seen that the conductivity increases with the increase of temperature. This type of variation indicates the semiconducting behavior of the films. The conductivity also increases with the increasing of Ni concentration.

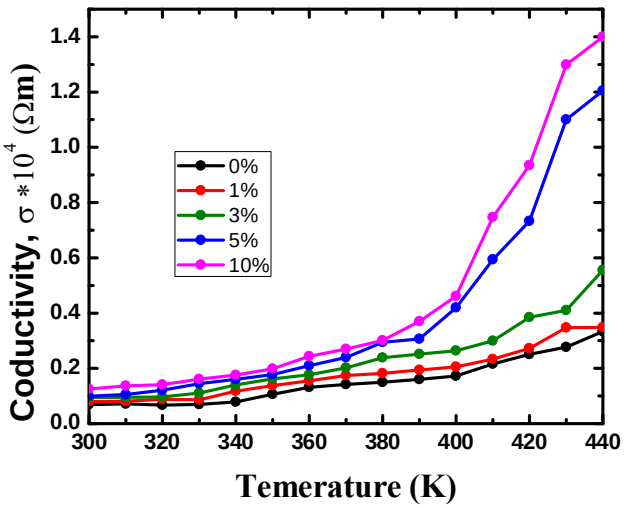

Fig 5.14.: Variation of electrical conductivity with temperature for as deposited thin films

5.6.3 Activation Energy Measurement

The variation of lnσ with inverse temperature of $Zn_{1-x}Ni_xO$ thin films is shown in fig. (5.15). The activation energy may be obtained by the relation

$$\sigma = \sigma_0 \exp\left(-\frac{\Delta E}{kT}\right) \qquad 5.5$$

Where ΔE is the activation energy, k is the Boltzmann constant and σ_o is the pre-exponential factor. From the slope of lnσ vs 1/T plot, the activation energy was

calculated [13]. Following this relation the activation energy of the films in were calculated from the slope of the plots.

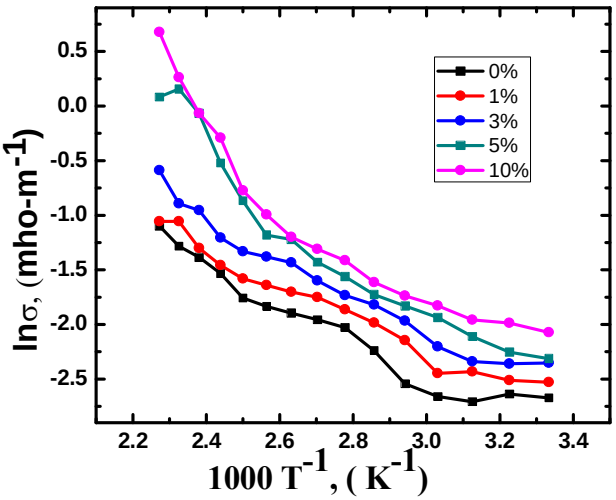

Fig. 5.15: Variation of lnů with 1/T for pure and Ni doped ZnO thin films.

Table 4: Variation of activation energy with doping concentration of $Zn_{1-x}Ni_xO$ films.

Sample	Concentration of Ni (wt %)	Activation energy φE (eV)
$Zn_{1-x}Ni_xO$	0	0.6838
	1	0.7924
	3	0.6607
	5	0.4177
	10	0.4639

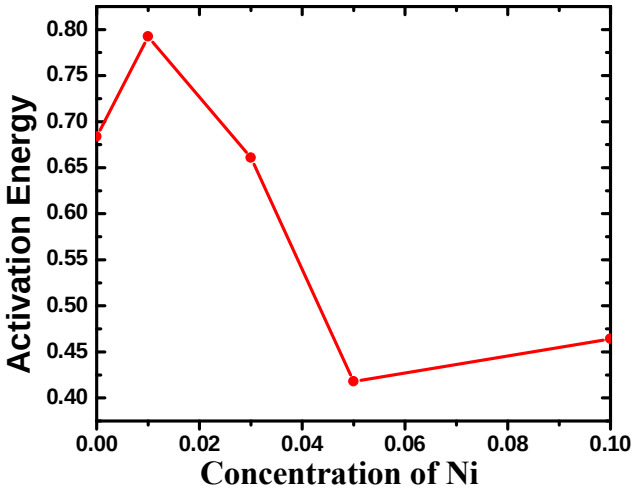

Fig. 5.16: Variation of activation energy (eV) of Ni doped ZnO thin films.

From the figure the 5% of nickel concentration the activation energy is smaller compared with other sample. These low values may be associated with the localized levels hopping due to the excitation of carriers from donor level to the conduction band.

References

1. Kaneva N. V., and Dushkin C. D., ñPreparation thin films of ZnO by sol-gel dip coatingò Bulgarian Chem. Com., Vol. 43, No. 2, P. 259-263, 2011.

2. Elilarassi R., And Chandrasekaran R., ñSynthesis and optical properties of Ni-doped zinc oxide nanoparticles for optoelectronic applicationsò Optoelectronics Lett., Vol.6, No.1, 2010.

3. Srinivas K., Manjunath Rao. S. And Reddy V., ñPreparation and properties of Zn0.9Ni0.1O diluted magnetic semiconductor nanoparticlesò J Nanopart Res, Vol.13, P. 817ï 837, 2011.

4. Kang S. J., Joung Y. H., Shin H. H., Yoon Y. S., òEffect of substrate temperature on structural, optical and electrical properties of ZnO thin films deposited by pulsed laser depositionò J. Mater. Sci.: Mater Electron, Vol. 1, P. 1073ï 1078, 2008.

5. Ohapatra j., Mishra D. K., Kamilla S. K., Medicher, B. R. R., Phase, D. S., and Singh, S. K., Ni-doped ZnO: Studies on structural and magnetic propertiesò Phys. Stat. Solid, Vol. 248, No. 6, P. 1352ï 1359, 2011.

6. Zhao R. B., Hou D. L., Guo J. M., Zhen C. M., and Tang G. D., ñRoom Temperature Ferromagnetism in Ni Doped ZnO Powdersò J. Supercond. Nov Magn., Vol. 23, P. 1261-1265, 2010.

7. Chauhan, Kumar A., and Chaudhary R. P., ñStructure And Optical Properties of $Zn_{1-X}Ni_xo$ Nanoparticles By Coprecipitation Methodrubyò J. of Optoelectronics and Biom. Mater., Vol. 3, Issue 1, P. 17-23 , 2011.

8. Maiti U. N., Ghosh P. K., Ahmed S. F., Mitra M. K., and Chattopadhyay K. K., ñStructural, optical and photoelectron spectroscopic studies of nano/micro ZnO:Cd rods synthesized via sol-gel routeò J. Sol-Gel Sci. Techn., Vol. 41, P. 87ï 92, 2007.
9. Elilarassi R., and Chandrasekaran G., ñSynthesis, structural and optical characterization of Ni-doped ZnO nanoparticlesò J. Mater. Sci.: Mater. Electron, Vol. 22, P. 751ï 756, 2011.

10. Buba A. D. A., and Adelabu J. S. A., ñOptical and Electrical Properties of Chemically Deposited ZnO Thin Filmsò. The Pacific J. of Sci. and Technol., Vol. 11, Num. 2, 2010.

11. Paul R. and Pal A. K. ñNi-DLC Composite Films Prepared by CVD Technique: Synthesis and Characterizationò Adv. Sci. Lett., Vol. 3, P. 323ï 332, 2010.

12. Singh S., Rama N. and Raoa M. S. R., ñInfluence of d-d transition bands on electrical resistivity in Ni doped polycrystalline ZnOò Appl. Phys. Lett., vol. 88, P. 222111, 2006.

13. Tewari S., and Bhattacharjee A., ñStructural, electrical and optical studies on spray-deposited aluminium-doped ZnO thin filmsò Pramana J. Phys., Vol. 76, No. 1, P. 153ï 163, 2011.

CHAPTER- VI

CONCLUSIONS AND SUGGESTIONS FOR FUTURE WORK

CHAPTER- VI

CONCLUSIONS AND SUGGESTIONS FOR FUTURE WORK

6.1 Conclusions

In the present work, ZnO and Ni-doped ZnO thin films were prepared by spray pyrolysis method. Films of different doping concentration of Ni were deposited on glass substrate keeping the substrate temperature at 300^0C. Different physical properties such as structural, optical and electrical properties have been studied.

It is observed that the nature of the deposited ZnO films depends on various parameters such as substrate temperature, concentration of the solution, spray rate and deposition time. Film deposited at 300^0C substrate temperature is found to be good in terms of their uniformity of thickness and colour. From the SEM micrograph thin films were found uniform and well covered on the glass substrate surface. Under higher magnifications, the SEM micrograph of the ZnO films shows smooth ganglia like fiber around the nucleation center. The Ni doped ZnO films also shows that pattern and the volume and size of fibers depends Ni. The average length of the fiber varies from 2.0 ε m to 2.5 ε m. The EDX analysis corresponding to Zn and O peaks of the spectrum, which confirms the ZnO thin film. For different concentrations of Ni in the film, there is also Ni peak in the spectra. EDX result reveals that the deposited films are very close to the nominal composition.

XRD was taken on as deposited $Zn_{1-x}Ni_xO$ thin films. XRD results show that as deposited film is mostly polycrystalline in all cases. Peaks have been identified for samples and from the position of peaks it is concluded that the structure is hexagonal wurtzite crystal structure. Lattice constant is calculated a = 3.2195Å and c= 5.1661Å. This value is quite close to the reported value. A secondary phase of NiO has been observed in higher Ni concentration sample excess of Nickel.

Absorption coefficient for ZnO and Ni doped ZnO have been calculated from transmission and reflection spectra taken within the wavelength of 250 nm to 1100 nm. The band gap was evaluated from the absorbance data. The band gap energy varies from 3.38 eV to 2.80 eV with doping concentration of the thin films. The observed value of band gap is found to be in good agreement with the value reported by others.

The electrical resistivity measurements were made on number of films from the room temperature up to 440K. The figure shows that the resistivity gradually decreases with the increase of temperature, which indicates the semiconducting nature of the materials. Resistivity also decreases with the increasing doping concentration. Conductivity has been calculated from resistivity measurements. The room temperature resistivity of the films decreases with increasing Ni and is found to be 14.48×10^{-3}, 12.55×10^{-3}, 10.52×10^{-3}, 10.12×10^{-3} and 7.95×10^{-3} mho $m^{\bar{1}\,1}$ for x = 0%, 1%0, 2%, 5% and 10%, respectively. At 440K temperature the resistivity of the films is found 2.99×10^{-3}, 2.87×10^{-3}, 1.80×10^{-3} , 0.91×10^{-3}, and 0.50×10^{-3} mho $m^{\bar{1}\,1}$ for x = 0%, 1%0, 2%, 5% and 10%, respectively.

In this study, the results obtained from optical, electrical and structural measurements are found to be in good agreement with the results obtained by previous worker on this material.

6.2 Suggestions for Future Work

This is the first time that Ni-doped Zinc oxide thin films have been prepared in our laboratory. We have deposited Zinc oxide and Ni-doped Zinc oxide thin films on glass substrate at 300^0C substrate temperature and studied some of their structural, electrical and optical properties. To prepare high quality films and their characterization more works are necessary, such as:

i) Study of the magnetic properties.

ii) Study of temperature dependence Hall effect.

iii) Study of electrical properties at low temperature.

APENDIX

Optical Data

Table1: Absorbance data for $Zn_{1-x}Ni_xO$ thin films

Wl	x=0%	x=1%	x=3%	x=5%	x=10%	x=15%
1100	0.15587	0.1364	0.11033	0.0792	0.06833	0.06193
1080	0.1592	0.13927	0.11253	0.08087	0.06947	0.06273
1060	0.16253	0.142	0.11473	0.08287	0.0708	0.06353
1040	0.16607	0.14493	0.1172	0.08487	0.07227	0.06453
1020	0.1678	0.14633	0.11833	0.08567	0.07293	0.06467
1000	0.17013	0.14813	0.11987	0.08727	0.0742	0.0654
980	0.17247	0.14993	0.12133	0.08887	0.07553	0.066
960	0.17467	0.15153	0.12273	0.0904	0.0768	0.0666
940	0.17667	0.15293	0.12387	0.09187	0.07807	0.06707
920	0.17873	0.15427	0.12493	0.09333	0.0792	0.0676
900	0.1808	0.15573	0.12607	0.0948	0.08067	0.0682
880	0.1832	0.15733	0.12727	0.0966	0.082	0.06893
860	0.18547	0.1588	0.12833	0.0982	0.0834	0.06973
840	0.1874	0.16007	0.12907	0.09987	0.08467	0.07013
820	0.19013	0.1616	0.13027	0.102	0.08633	0.0712
800	0.19253	0.16327	0.1314	0.10387	0.08773	0.07213
780	0.1952	0.16453	0.13267	0.10613	0.08953	0.07307
760	0.19807	0.1664	0.1338	0.109	0.0912	0.0744
740	0.2014	0.16813	0.1352	0.11147	0.09233	0.07527
720	0.20467	0.16987	0.13673	0.1132	0.09287	0.0756
700	0.20873	0.17207	0.139	0.1172	0.09393	0.077
680	0.2152	0.1744	0.1428	0.1312	0.09893	0.08413
660	0.2222	0.17713	0.14673	0.14427	0.10407	0.09147
640	0.22593	0.1802	0.14867	0.14333	0.10333	0.08967
620	0.23093	0.1834	0.1518	0.14907	0.10547	0.09153
600	0.2346	0.187	0.15413	0.14813	0.10533	0.08953
580	0.23973	0.19093	0.15773	0.15293	0.10807	0.09107
560	0.247	0.19567	0.16233	0.16127	0.11313	0.0948
540	0.25653	0.2012	0.16847	0.17627	0.12153	0.10227
520	0.26853	0.20687	0.17673	0.2014	0.13447	0.11653
500	0.28513	0.21387	0.18807	0.23647	0.15187	0.13687
480	0.3056	0.2222	0.20167	0.2792	0.17153	0.22793
460	0.33047	0.233	0.21733	0.3256	0.25867	0.32027
440	0.33907	0.24753	0.2348	0.43867	0.3462	0.479
420	0.33733	0.274	0.26033	0.4998	0.5056	0.7512
400	0.36711	0.3062	0.39	0.7358	1.0358	1.2696
380	0.4218	0.39147	0.78553	1.2688	1.51173	1.6588
360	0.50447	0.75707	1.1338	1.67487	1.89087	2.07087
340	0.93907	1.22047	1.50173	2.03993	2.26947	2.40207
320	1.3002	1.54853	1.8374	2.41487	2.5402	2.73767
300	1.66833	2.16087	2.2036	2.8302	2.90447	3.06753
290	1.3268	1.83013	2.63693	3.10687	2.51247	3.27273

Table2: Transmittance data for $Zn_{1-x}Ni_xO$ thin films

Wl	x=0%	x=1%	x=3%	x=5%	x=10%	x=15%
1100	62.46	65.04	67.88	73.54	78.91	80.66
1080	61.89	64.42	67.38	73.08	78.59	80.47
1060	61.3	63.76	66.87	72.61	78.25	80.22
1040	60.69	63.01	66.31	72.11	77.87	79.96
1020	60.41	62.65	66.09	71.95	77.67	79.92
1000	60.03	62.12	65.75	71.66	77.34	79.74
980	59.68	61.66	65.43	71.37	77.01	79.57
960	59.34	61.19	65.11	71.12	76.66	79.38
940	59.05	60.78	64.87	70.91	76.35	79.26
920	58.76	60.36	64.62	70.73	76.01	79.11
900	58.48	59.91	64.38	70.52	75.67	78.96
880	58.15	59.46	64.12	70.3	75.29	78.76
860	57.86	59	63.88	70.1	74.94	78.58
840	57.62	58.54	63.7	70	74.65	78.43
820	57.3	58.01	63.42	69.75	74.21	78.14
800	56.98	57.48	63.16	69.57	73.48	77.91
780	56.7	56.92	62.9	69.34	73.4	77.65
760	56.37	56.32	62.63	69.09	72.97	77.31
740	56.03	55.73	62.33	68.84	72.69	77.05
720	55.68	55.09	62	68.57	72.58	76.98
700	55.27	54.35	61.54	68.1	72.31	76.61
680	54.82	53.5	60.74	67.24	71.04	74.77
660	54.3	52.59	59.9	66.37	69.8	72.91
640	53.72	51.81	59.51	66.05	69.98	73.36
620	53.13	50.95	58.89	65.45	69.47	72.89
600	52.47	50.04	58.44	65.05	69.51	73.4
580	51.75	49.06	57.7	64.37	68.84	73.02
560	50.89	47.95	56.8	63.46	67.66	72.09
540	49.94	46.7	55.59	62.22	65.77	70.24
520	48.95	45.26	53.97	60.5	62.89	66.89
500	47.75	43.57	51.89	58.23	59.27	62.4
480	46.41	41.54	49.48	55.57	55.37	57.37
460	44.69	39.12	46.78	52.6	51.53	52.48
440	42.49	36.25	44.03	49.54	47.9	48.01
420	38.81	31.71	40.3	45.52	43.75	42.81
400	30.29	22.38	32.35	37.28	35.18	31.32
380	12.68	7.62	15.98	19.93	17.08	10.27
360	2.78	1.34	4.41	5.62	2.91	0.65
340	1.9	0.82	2.58	2.76	0.46	0.05
320	1.99	0.71	1.26	1.28	0.1	0
300	0.99	1.15	0.62	0.7	0.07	0.05
290	0.56	8.3	4.2	0.4	0.08	0.5

Table3: Electrical data for temperature dependent resistivity $Zn_{1-x}Ni_xO$ thin film sample
Substrate temperature = 300°C
Doping concentration of Ni =0%

Temperature in K	T^{-1}in $k^{-1}*10^{-3}$	Resistivity ɟ in ohm-m$*10^{-3}$	Conductivity ů =1/ɟ $*10^{4}$ in mho-m^{-1}
300	3.33333	14.48881	0.06902
310	3.22581	13.96517	0.07161
320	3.125	15.00935	0.06663
330	3.0303	14.30445	0.06991
340	2.94118	12.70525	0.07871
350	2.85714	9.39156	0.10648
360	2.77778	7.60576	0.13148
370	2.7027	7.0685	0.14147
380	2.63158	6.66211	0.1501
390	2.5641	6.25791	0.1598
400	2.5	5.7989	0.17245
410	2.43902	4.63442	0.21578
420	2.38095	3.99334	0.25042
430	2.32558	3.60867	0.27711
440	2.27273	2.99919	0.33342

Table4: Electrical data for temperature dependent resistivity for Ni doped ZnO thin film sample.
Substrate temperature = 300°C
Doping concentration of Ni =1%

Temperature in K	T^{-1}in $k^{-1}*10^{-3}$	Resistivity Ɉ in ohm-m$*10^{-3}$	Conductivity ů =1/Ɉ $*10^{4}$ in mho-m^{-1}
300	3.33333	12.53837	0.07976
310	3.22581	12.32178	0.08116
320	3.125	11.38954	0.0878
330	3.0303	11.55167	0.08657
340	2.94118	8.53898	0.11711
350	2.85714	7.27553	0.13745
360	2.77778	6.44339	0.1552
370	2.7027	5.75557	0.17374
380	2.63158	5.48632	0.18227
390	2.5641	5.1611	0.19376
400	2.5	4.86	0.20576
410	2.43902	4.29255	0.23296
420	2.38095	3.6705	0.27244
430	2.32558	2.87618	0.34768
440	2.27273	2.87328	0.34803

Table5: Electrical data for temperature dependent resistivity for Ni doped ZnO thin film sample.
Substrate temperature = 300°C
Doping concentration of Ni =3%

Temperature in K	T^{-1}in $k^{-1}*10^{-3}$	Resistivity ɟ in ohm-m$*10^{-3}$	Conductivity ů =1/ɟ $*10^{4}$ in mho-m^{-1}
300	3.33333	10.52433	0.09502
310	3.22581	10.58426	0.09448
320	3.125	10.37425	0.09639
330	3.0303	9.04422	0.11057
340	2.94118	7.1482	0.1399
350	2.85714	6.16613	0.16218
360	2.77778	5.65612	0.1768
370	2.7027	4.94212	0.20234
380	2.63158	4.19408	0.23843
390	2.5641	3.9768	0.25146
400	2.5	3.79209	0.26371
410	2.43902	3.34308	0.29913
420	2.38095	2.59891	0.38478
430	2.32558	2.43985	0.40986
440	2.27273	1.80138	0.55513

Table6: Electrical data for temperature dependent resistivity for Ni doped ZnO thin film sample.
Substrate temperature = 300°C
Doping concentration of Ni =5%

Temperature in K	T^{-1}in $k^{-1}*10^{-3}$	Resistivity ɟ in ohm-m$*10^{-3}$	Conductivity ů =1/ɟ $*10^{4}$ in mho-m^{-1}
300	3.33333	10.11611	0.09885
310	3.22581	9.51572	0.10509
320	3.125	8.25573	0.12113
330	3.0303	6.93854	0.14412
340	2.94118	6.22927	0.16053
350	2.85714	5.62254	0.17786
360	2.77778	4.76653	0.2098
370	2.7027	4.17445	0.23955
380	2.63158	3.39438	0.2946
390	2.5641	3.26193	0.30657
400	2.5	2.38554	0.41919
410	2.43902	1.6849	0.59351
420	2.38095	1.07146	0.83331
430	2.32558	0.8547	1.07
440	2.27273	0.91869	1.08851

Table7: Electrical data for temperature dependent resistivity for Ni doped ZnO thin film sample.
Substrate temperature = 300°C
Doping concentration of Ni =10%

Temperature in K	T^{-1}in $k^{-1}*10^{-3}$	Resistivity ɟ in ohm-m$*10^{-3}$	Conductivity ů =1/ɟ $*10^{4}$ in mho-m^{-1}
300	3.33333	7.95015	0.12578
310	3.22581	7.29556	0.13707
320	3.125	7.09228	0.141
330	3.0303	6.22459	0.16065
340	2.94118	5.68741	0.17583
350	2.85714	5.02866	0.19886
360	2.77778	4.10826	0.24341
370	2.7027	3.702	0.27012
380	2.63158	3.31888	0.30131
390	2.5641	2.70535	0.36964
400	2.5	2.16639	0.4616
410	2.43902	1.3383	0.74722
420	2.38095	1.06903	0.99543
430	2.32558	0.7698	1.19904
440	2.27273	0.5076	1.27006